Thermal Science and Engineering Progress 60 (2025) 103258

Contents lists available at ScienceDirect

Thermal Science and Engineering Progress

journal homepage: www.sciencedirect.com/journal/thermal-science-and-engineering-progress

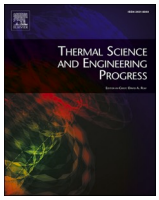

Modeling and optimization of energy efficiency and product quality in staple food roasting using machine learning: A case study on cassava processing

Mwewa Chikonkolo Mwape [a,*], Boris Kulig [a], Tina Nurkhoeriyati [b], Franz Roman [a], Aditya Parmar [c,e], Naushad M. Emmambux [d], Oliver Hensel [a]

[a] Department of Agricultural and Biosystems Engineering, University of Kassel, Nordbahnhoftstraße 1a, Witzenhausen 37213, Germany
[b] Food Technology Department, Faculty of Engineering, Bina Nusantara University, Jakarta 11480, Indonesia
[c] International Center for Living Aquatic Resources Management (ICLARM-WorldFish), Penang, Malaysia
[d] Department of Consumer and Food Sciences, University of Pretoria, Private Bag X20, Hatfield 0028, South Africa
[e] Natural Resources Institute, Central Avenue, Chatham Maritime, Kent, ME4 4TB, UK

ARTICLE INFO

Keywords:
Roasting prediction models
Machine learning modeling
Energy efficiency
Data-Driven Design
Post-Harvest
I-Optimal designs

ABSTRACT

Energy-efficient food processing techniques, including roasting could help reduce post-harvest losses which currently exceed 30 % annually. Roasting enhances food dehydrated for extended shelf life and quality. In most developing countries, roasting is drudgery, nutrient altering, unsustainable and mostly woodfuel powered. Lack of optimized important process factors such as temperature and agitation speed, presents a significant challenge in achieving process and energy efficiency, Therefore this research sought to bridge these gaps by modeling and optimizing the temperature/Rate of Rise (RoR) and agitation speed at standard quality of the roast using fresh cassava processing into cassava-pulp as a case study. The Machine Learning (ML)-Integrated Design; I-Optimal Response Surface Methodology (RSM) and Random Forest (RF-Python) techniques with two factors (temperature (90–250 °C and agitation speed-10–50 RPM) and seven responses, were used for experimental design, modeling, optimization, prediction of design parameters for real-life application in a solar PV roaster and model validation. External validation was reinforced with python driven Mann-Whitney U, Levene and Bland-Altman tests. The optimum parameters where find to be; 130 °C-roasting temperature with 21.08 °C min^{-1}-RoR, 40 RPM, 22.27 min, 1.37 kWh $kg\text{-}gari^{-1}$-Specific-Energy-Consumption (SEC), color-(74.55-L^*, 2.97-a^*, −23.98-b^*), 3.40-swelling index-(SI), and 1.36 mm-texture. The models predicted the real-life Solar-PV roasting system design parameters with accuracy above 90 %, Mean-Absolute-Error (MAE-0.99) and showed significant SEC savings of 81.40 % against the 7.37 kWh $kg\text{-}gari^{-1}$ woodfuel-based-cookstove. This scalable, data-driven solution could be applied to design and develop more efficient and high-quality roasting systems. Future studies should focus on generalizing with different staple foods.

1. Introduction

Globally, over 30% of food produced (US$1 trillion) succumbs to post-harvest losses annually due to insufficient preserving and storage technology infrastructure mostly in developing countries [1]. Roasting and other processes involving heat can change the physicochemical and structural makeup of the food matrix for improved digestibility, taste and extending the shelf life of perishable foods like fresh cassava.

In the food industry, roasting is a popular thermal processing technique that improves the flavor, color, and texture of food products. The process includes complex chemical reactions such as the Maillard reaction, gelatinization and caramalization, which contribute to favorable physical appearance and sensory properties. The temperature control, agitation speed, and energy input are essential elements in maximizing both product quality and process efficiency [2–4].

There are several ways to roast food, such as traditional, pan, oven etc. The key distinctions between these methods are in how heat is applied and transferred [5]. The majority of developing countries employ pan-roasting techniques, which involve using clay, cast iron, or stainless steel cookware set atop open combustion chambers powered

* Corresponding author.
E-mail address: chikonkolo@uni-kassel.de (M.C. Mwape).

https://doi.org/10.1016/j.tsep.2025.103258
Received 10 August 2024; Received in revised form 6 December 2024; Accepted 12 January 2025
Available online 23 January 2025

primarily by woodfuel—a resource that is getting harder to find and raises concerns about deforestation and greenhouse gas emissions. Pan roasting systems are conductive in nature, and continuous agitating or mixing ensures uniform and quick distribution of heat.

Usually, characteristics including color, moisture content, swelling index, particle size, and pH are used to evaluate the final products quality. These factors impact the texture, flavor, and customer acceptability of the products, making them important markers of the roasting process efficacy. For example, the maillard reaction directly results in color, whereas texture and shelf life is influenced by moisture content. Furthermore, factors like swelling index and particle size affect the roasted product's texture and physical characteristics. Therefore, in addition to process optimization, a thorough roasting technique must take these quality attributes in perspective.

Moreover, roasting is considered as energy intensive, complicated, highly non-linear process and involves complex mechanisms such as physical, chemical, and metabolic interactions, similar to other drying techniques and despite extensive research, significant gaps remain in understanding the combined effects of these mechanisms, particularly when applied to different food matrices [5,6].

Several researchers have investigated the effects of roasting settings of different food products. Table 1 summarizes major finding from recent work, emphasizing both focal areas and identified gaps.

Table 1 shows that all studies identified temperature and time as significant parameters in roasting, stressing their involvement in promoting chemical processes such as Maillard and gelatinization. For example, all of the researchers indicated that roasting respective food products at medium to high temperatures reduces the time it takes to increase the production of the desirable taste components. Research on energy optimization in roasting, such as that conducted by Rahayuningtyas et al., [18] mostly focused on lowering energy usage while maintaining product quality by mainly adjusting temperature profiles. Furthermore, studies by [10–12,16] that focused solely on temperature, energy and time may have overlooked other influential factors such as agitation, which is critical in ensuring even heat dispersion at standard quality parameters. Agitation speed has a direct impact on heat transfer efficiency and homogeneity and Sruthi et al [5] found that it is important for preventing over- or under-roasting, especially in larger food items like coffee beans and seeds. The total quality, consistency, cost of production and market value of finished products may be altered by uneven roasting induced solely by temperature and time optimization [19,20].

Despite insightful observations, there are significant gaps in the literature, especially with regard to the holistic analysis of the combined effects of energy efficiency and inputs, agitation speed, temperature and the final products quality and visual parameters (color, moisture content, swelling index, particle size, and *pH etc.*). Most studies as highlighted in Table 1 tend to focus on isolated factors without exploring their interactions, which are crucial for products like nuts, roots, grains, tubers and seeds that require uniform roasting to achieve shelf and high quality stability.

There has been lack of comprehensive studies exploring holistic optimization in specific high-moisture and perishable foods like cassava. Fresh cassava with 45 to 80% wet basis moisture content is one of the high-rate perishable tropical crops and should be processed into shelf and quality stable products within two days after harvesting [21].

Cassava has been termed "the drought, war, and famine resistant crop" due to its ability to grow in harsh conditions, such as soils with low fertility and conflict-affected areas [22]. Its flexibility to be harvested when needed rather than only at the end of the growing season emphasizes its ability to provide a food reserve in times of hunger and conflict. It is the primary source of calories for more than 300 million people in Sub-Saharan Africa (SSA). Roughly 75% of the cassava cultivated in Africa is processed into gari, grated, sieved and a semi-gelatinized cassava product (pulp) [21]. Furthermore, it has been proposed that when compared to other significant agricultural products, cassava may be more resistant to climate change [23].

Cassava presents distinct challenges and opportunities for roasting optimization. Even if in some sectors cassava roasting is referred to as cassava frying, scientifically frying involves the immersing of food in hot oil at between 160 °C and 200 °C allowing rapid heat transfer through conduction from the oil to food, while roasting does not involve oil [24,25]. And in the research area considered in this study, oil was not added during gari roasting. Unlike seeds, coffee etc., fresh grated cassava mash's high moisture content in its colloidal suspension state, is a safe haven of cyanogenic glycosides which can release toxic hydrogen cyanide if not properly handled. The high moisture content of the cassava mash also promotes organism growth for accelerated spoilage [26]. Therefore, the following factors distinguish the roasting procedure for cassava in its requirements from other roastable staple food products such as rice and sorghum:

- **Energy input:** Cassava has high moisture content, thus roasting it with optimum energy is crucial to cutting down on drying time and processing expenses.
- **Temperature regulation:** Ensuring enough heat to deactivate hazardous chemicals while avoiding charring or over roasting is critical for producing safe cassava products such as gari.
- **Agitation speed:** Achieving consistent drying and roasting requires effective agitation, which is essential for distributing the moisture content uniformly among the cassava mash.

Table 1
Overview of recent research on food roasting.

Type of food	Roasting temperature (°C)	SEC (kWh kg^{-1})	Agitation speed (RPM)	Duration (min)	Methods/Factors	Gap	References
Maize	160–240	N/A	80	10–50	Temp and Time (Electric roaster) RSM	Energy not indicated	[7]
Groundnuts	140–200	0.4–3	4.5–19	10–90	Temp and moisture (Electric roaster)-RSM	Quality metrics not indicated	[8,9]
Almonds	129–155	1.95–5.42	N/A	10–55	Temp and nut microstructure (hot air oven) Two step roasting process	Agitation speed not indicated	[10,11]
Soybean	110–130	N/A	N/A	20–120	Temp and time (Electric oven)-ANOVA	Energy and agitation speed not indicated	[12,13]
Coffee	150–250	0.35–0.95	40–80	3–20	Fluidized-bed, drum roasters		[14]
Gari	110–256	N/A	N/A	9–17	Batch size, physiochemical properties, temp (Wood cookstove) PCA	Energy not considered and stirring speed was indicated as a fraction of the total roasting time	[15]
Gari	110–142	7.37	N/A	9–21	Energy efficiency, batch size and temp(wood cookstove)	Agitation speed not indicated	[16]
Gari	80–85	N/A	N/A	30–35	Processing methods (3 stone wood cookstoves)	Agitation speed not indicated	[17]

N/A = Not available, RSM = Response Surface Methodology, ANOVA = Analysis of Variance, PCA = Principal Component Analysis.

- **Quality of the final product:** Color, test, particle size and swelling index are all critical quality and visual parameters important and determined by process temperature and agitation speed [27].

According to the literature examined, optimization of the temperature with its Rate of Rise (*RoR*), stirring speed (agitation), and time and energy consumption during the roasting procedures of most foods in relation to quality attributes such as color, swelling index, and texture is scarce. There are also limited data reported on the fitting of the Moisture Ratio (MR) of the roasting processes to most of the existing drying kinetic models, such as the Midilli-Kucuk and Page etc., which are important for roasting data validation and process efficiency [28,29]. More so, the *RoR*, a critical technique that acts like a roasting process "Tachometer", is lacking in most of the food processing techniques apart from coffee [30,31]. Knowledge of *RoR* is essential for enhancing roasting profiles (by equipment and process design) and ensuring the qualitative and quantitative sustainability of the finished products. With the fast shift and demand to transition to Industry 4.0 and the need of a sustainable recover from Covid-19 in the eye of climate change mitigation, where AI and machine learning have taken a center stage, optimized models such as agitation speeds, temperature bands, *RoR*, specific energy consumption, and qualitative and quantitative metrics are critical [32–34].

The process of creating new innovations in roasting processes is made difficult and inefficient by the lack of comprehensive data on the optimized roasting process parameters for the majority of roasting procedures, including roasting of cassava into gari. The implementation of the energy transition from non-renewable sources is negatively impacted by this aspect [35]. Optimization of multiple parameters in food processing systems presents several challenges from complex interactions, trade-offs, data management, costs and regulatory, and traditional (ethnic) compliance to variability. These challenges require a calculated balance that often involve the application of sophisticated techniques like statistical models, machine learning (ML) and most recently, digital twins to effectively manage and optimize the parameters [36].

One way to address the complications of multiple metrics and optimizing the roasting processes is by employing the Response Surface Methodology (RSM). RSM is a sophisticated statistical technique for modeling and analyzing the effects of several independent variables and interactions and has been used by many researchers in food sciences as highlighted in Table 1 [7–9]. For the roasting processes, RSM integrated with ML-based modeling tools could offer a robust framework to explore variable interactions of the temperature, agitation speed and energy input on quality attributes as reported on other processes [37]. Integration of RSM with ML tools could ensure accuracy in equipment design and development thereby ensuring energy efficiency while achieving desirable quality and provides data driven insights that could be translated into actionable recommendations for improving industrial scale roasting processes sustainability. The developed scripts for example in python could be used in Artificial Intelligence (AI) tools for efficient and sustainable roasting process automation.

Therefore, this study was commissioned to investigate and optimize the temperature and agitation speed at optimum energy, roasting time, and standard quality parameters during the roasting process using cassava roasting into gari as a case scenario. This was achieved by mimicking the traditional cassava processing techniques monitored from some women cooperatives in the Maritime region, Togo. The optimized data (models) were pre-processed and feature engineered, trained and then domain adapted to fit the real-life cassava roasting conditions based on Maritime region conditions in Togo (ambient/initial temperatures, and popular roasting pan dimensions). The prediction models (lab-scale) and separate real-life data validation was performed via the developed roasting process specific Bland-Altman external validation integrated python scripts.

To achieve the above, the following specific objectives where adopted:

1. To model the roasting process of cassava: Evaluating the effects of agitation speed, and temperature on the specific energy consumption and product quality attributes.
2. To optimize roasting parameters: Optimization of the cassava roasting process (temperature, energy, stirring speed, time) for optimal quality (color, particle size, and swelling index) and minimum power consumption.
3. Conduct a dynamic heat and mass transfer models for the lab-scale roasting process.
4. To predict the design parameters for the commonly used roasting pans in Togo's Maritime region and validate the predictive models using the real-life experimental data providing recommendations for industrial scale cassava roasting

This work highlights the significance of applying theoretical models created under lab-scale conditions to real-world applications where intricacy and unpredictability of field and site specific conditions necessitate reliable and site customized solutions. It reinforces dependable deployment of research works in dynamic, real-life systems by bridging the gap between predictions made in controlled environments and actual field performance through the use of machine learning techniques and python-based tools for model optimization, design parameters prediction, training and validation.

2. Methods and materials

2.1. Raw materials

The sweet and white fresh cassava imported from South America (Costa Rica) purchased in October 2022 from an Asian shop in Frankfurt, Hessen- Germany, was used as for the experiments.

2.2. Sample preparations

The cassava was carefully peeled using lab knives and cut into small pieces before being grated with a kitchen food chopper (HOVOBO Food Processor, 500 W electric meat grinders, HOVOBO, China). A hydraulic press was used to dewater the cassava mash, which was then sifted by hand before sieving with a laboratory vibrator (Eijkelkamp VS 1000, Royal Eijkelkamp B.V., Giesbeek, The Netherlands) equipped with a train of various sieve sizes (0.5 to 8 mm was used). The samples were left for a day-(24 h) to ferment. The processes mimicked the traditional cassava preparations observed in Togo and mentioned in the literature [38,39].

2.3. Experimental design

The varied experimental and optimization parameters (temperatures and stirring speeds) were chosen based on multiple preliminary tests carried out at University of Kassel laboratories and material and energy flow analysis carried out from selected small-scale gari processors in Lome, Togo and reviewed literature [38,40]. This method has been applied and reported by other researchers [41].

I-Optimal design of two factors (Temperature and agitation speed) by 25 runs comprising of nine responses (time (Y_1), energy (Y_2) final moisture content (Y_3), color components (L^* (Y_4) b^*(Y_5) and a^* (Y_6)) *pH* (Y_7), swelling index (SI) (Y_8) and texture (Y_9)) with five replicated runs. Nevertheless, it was discovered that the initial and final moisture contents, as well as pH, were very comparable; hence they were overlooked during model fitting and optimization. Data analysis/optimization was performed by integrating python and ML tools with JMP data analysis software [42]. The cassava mash feeding was run at the maximum roasting pan capacity of 0.3 kg per run. A run was considered complete at 10.2% moisture content measured using a calibrated moisture meter

and verified using the American Association of Cereal Chemists' technique of analysis (AACC) in % method 44–19.01[43]. To keep the moisture content of all cassava mash samples consistent before roasting, peeling and grating were staggered to guarantee that only the samples needed on that day were processed to 48.6% moisture content. The samples were kept at a nearly constant moisture level using the humidity chamber. There was minor moisture variations ranging from 0.2 to 0.8%, which could be attributed to the time spent loading the samples into the dryer for moisture content analysis or on roasting.

The applied roasting temperatures ranged from 90 to 250 °C, with the number of replications per temperature level as follows: 5 at 250 °C, 7 at 210 °C, 2 at 170 °C, 7 at 130 °C and 7 runs at 130 °C. The stirring speed ranged from 10 to 50 revolutions per minute (RPM), with five runs at 10 RPM, seven at 20 RPM, two at 30 RPM, seven at 40 RPM and four at 50 RPM as highlighted in Appendix A.

Regression analysis was applied to the experimental data. The robust regression techniques involving the centering by the median and scaling by the Interquartile range (IQR) for a second-order polynomial Equation (1), were used to fit the model and predict the responses under optimum roasting conditions.

$$Y_i = \beta_0 + \beta_1\left(\frac{X_1 - x_1}{IQR(X_1)}\right) + \beta_2\left(\frac{X_2 - x_2}{IQR(X_2)}\right) + \beta_{12}\left[\left(\frac{X_1 - x_1}{IQR(X_1)}\right) \times \left(\frac{X_2 - x_2}{IQR(X_2)}\right)\right] + \beta_{11}\left[\left(\frac{X_1 - x_1}{IQR(X_1)}\right)^2\right] + \beta_{22}\left[\left(\frac{X_2 - x_2}{IQR(X_2)}\right)^2\right] + \varepsilon \quad (1)$$

where, X_1 and X_2 represented the two independent variables, temperature in degrees Celsius and stirring speed in RPM respectively. Y_1 denotes the responses, β_0 denotes the intercept term, β_1 and β_2 temperature and stirring speed linear coefficients respectively, β_{12} is interactions terms, β_{11}, and β_{22} are quadratic coefficients and script ε representing the errors. For the temperature median $=_{X_1}$ and for stirring speed $=_{X_2}$ while the Interquartile range for temperature $= IQR(X_1)$ and for stirring speed $IQR(X_2)$ [41,44–47].

The statistical significance of the regression coefficients was examined using the Analysis of Variance (ANOVA) at a 95% confidence level [6,41,44,48]. The coefficient of determination (R^2) was also used for verification.

2.4. Roasting process setup

Fig. 1 highlights the roasting process setup.

2.4.1. Lab-scale roasting pan details

An aluminum-cast electric Wok rated 230 VAC, 1850 to 2200 W with dimensions 0.22 x 0.42 x 0.42 m, was used as an Electric Roasting Pan (ERP). A 12 VDC-powered stirrer (CS) coupled with a digital LED Tachometer (ST) with an accuracy of ± 0.1% (4–30 DCV and 10–9999 RPM) was developed and optimized for these experiments.

2.4.2. Temperature control and data mining

With a self-tuning PID technology (Model YT-124, STEEIRO with ±0.5% digital display accuracy), the REX-C100 LED PID Temperature Regulator (TR) was connected to the primary power supply (PS). The TR got the set control temperature feed from TC2. The K-type thermocouples were utilized to detect temperature from various ERP points, as shown in Fig. 1 using the Fluke Hydra Data Logger 2620A Model (TDL) for subsequent storage on the Laptop (LC).

2.4.3. Energy and agitation speed data capture

The ERP drew power through a Voltcraft 4000 (3500W/15A Max.-230ACV) Energy Data Logger (EDL) via the TR-regulated Circuit Adapter (CA). The ERP's energy consumption data was captured every second using an SDHC card and an inbuilt data logger with ±1% +1 count efficiency. The data was then transferred to a computer for analysis. The CS with the ST indicator was used to achieve the various agitation speed settings of the de-watered cassava mash and gari. A Voltcraft SEM6000 with 1% accuracy was used for the CS energy data logging. The total energy consumption ($E_{C/R}$) in kWh per run was the sum of the ERP and CS consumption.

2.4.4. Mass, cut-out moisture content and time data capture

The ERP, CS, and ST sub-systems were arranged on top of the Digital Scientific Balance (DSB) (Sartorius GmbH, Göttingen, Germany) to track and record the mass change every minute of the run duration. The processed gari per run in kilograms (M_G) was used to denote the final

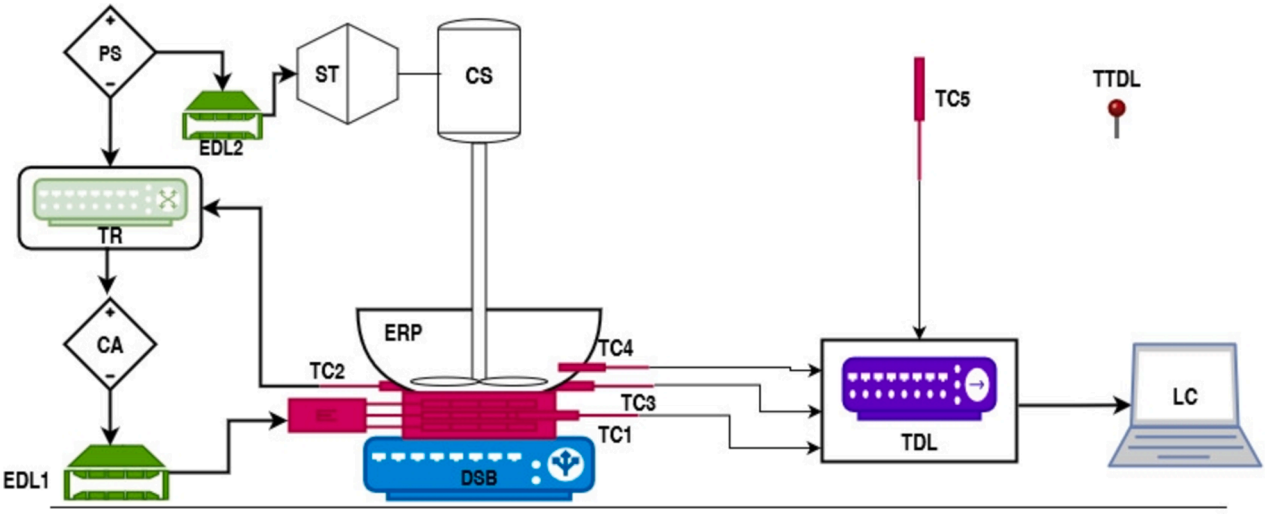

Fig. 1. Roasting process setup.

mass. An optimized hand held moisture meter (HE90, PFEUFFER GMBH, Flugplatzstrabe 70, 97,318 Kitzingen, Germany), was used to measure the final moisture content (10.2%) and was verified by thermogravimetric techniques as discussed [38].

The start and end times were recorded with a stopwatch. However, all data loggers include integrated time monitoring controls, which serve as a suitable backup.

2.4.5. Cassava roasting operation

Each run began when the weight of the 0.3 kg of cassava mash that was poured into the roasting pan was verified on the DSB. At the same time, the appropriate run temperature and agitation speed were adjusted. After setting the EDL1 and EDL2 to zero, all temperature sensors were examined. The PS was then turned on, and the time was noted. The moisture content at the end of the roasting process was fixed at 10.2%.

2.5. Specific energy consumption (SEC) and energy efficiency

The SEC in kWh kg^{-1} was computed as by dividing the total energy consumption ($E_{C/R}$) in kWh with the total gari produced (kg) for each batch (M_G) as shown in Equation (2) [49],

$$SEC_R = \frac{E_{C/R}}{M_G} \tag{2}$$

The energy efficiency was calculated as the ratio of the energy used over the total energy supplied to the roasting system [50].

2.6. Moisture content (MC), moisture ratio (MR) roasting time (R_t), cumulative rate of evaporation (RoEv) and rate of Rise (RoR)

The American Association of Cereal Chemists' technique of analysis (AACC) (method 44–19.01[43] was used to estimate the moisture content *(MC)* in % and calculated as initial moisture content as well as the *MC* at each stage of the roasting process using Equation (3);

$$MC = \left(\frac{W_x - W_z}{W_x}\right) \times 100 \tag{3}$$

where; W_x represent the Initial sample weight (kg) and W_Z was the dry weight of the sample at a specified time.

The moisture ratio *(MR)* at time *t* (min) and the *RoEV* where calculated using Equation (4) and (5) as highlighted below respectively.

$$MR = \frac{MC_t - MC_e}{MC_0 - MC_e} \tag{4}$$

$$RoEv = \frac{Cumulative\ water\ evaporated\ in\ specified\ time}{Cumulative\ time\ taken} \tag{5}$$

where MC_0 was initial *MC* dry basis, MC_t was *MC* at each stage, and time *dt* (min) on dry basis (time was recorded from the stopwatch) It was assumed that the equilibrium *MC* (MC_e) was negligible.

The *RoR* ($^oC\ min^{-1}$) was achieved by measuring how relatively temperature (^oC) changed with the roasting time (min) using Equation (6).

$$RoR = \frac{T_{t+dt} - T_t}{dt} \tag{6}$$

where; T_t (Cassava mash temperatures at time *t*) and T_{t+dt} (cassava mash temperature at time t+dt)). The time it took to heat the cassava mash to the new temperatures) signified changes in temperatures (Y axis in (^oC)) and time (X-axis in min) respectively. The *RoR* is a technique for tracking the rate of temperature change during roasting and could act like a "Tachometer" of the roasting process and might be beneficial in categorizing the roasting process for good quality of the end product [30,31,51,52].

2.7. Roasting process kinetics model fitting

By plotting the drying time against the moisture ratio, the drying kinetics curve of the optimized run was constructed. Then the mathematical models highlighted in Table 2 (More data in supplementary materials under Table 2), applied by different researchers, were fitted to the achieved *MR* for model predictions, understanding the roasting process dynamics and conditions optimization [28,29,53–55].

Determination of model coefficients and analysis of non-linear regression was achieved by using JMP version 16. In this work, the statistical error reefing approaches used to assess the models' correctness were the Mean Squared Error (MSE), the Root Mean Square Error (RMSE), and the Sum Squared Error (SSE) [54,60]. The lower the Sum Squared Error (SSE) at 0.05 significance level, the best fitted the model was regarded and selected using the following expression,

$$SSE = \sum_{i=1}^{n} \left(MR_t - MR_p\right)^2 \tag{7}$$

where MR_p, was the predicted moisture ratio.

2.8. Quality considerations

In this study, we evaluated the quality of gari based on color, swelling index, texture, and *pH*, as proxies of sensory taste (Appendix A). These factors, strongly associate with taste, and provide substantial insights. For example color influences the visual attractiveness and flavor anticipation [61], swelling index affects mouthfeel and flavor release [62], texture impacts sensory experience [63] and *pH* impacts the stability and flavor characteristics [64]. By assessing these parameters, aspects of taste can be inferred ensuring that the product meets general sensory expectations.

Furthermore, different regions, cultures, and groupings have varying sensory expectations for gari. For example, some regions prefer a lighter hue and a milder sour flavor, whilst others prefer a darker color and a sourer flavor [65]. These variations might cause discrepancies in product acceptance, demanding personalized approaches to match unique expectations while ensuring consumer happiness and market success. Future studies could embark on these gaps.

2.8.1. Chromaticity

The Chromameter (CR–400, Minolta Camera Co. Ltd., Osaka, Japan) was used to measure the chromaticity of gari in triplicates. This method where Commission International de l Eclairage (CIE) color attributes; L^* for the darkness (0) to whiteness (100), a^* for the redness to greenness, and b^* for blueness to yellowness, has been used by many researchers to determine changes in color attributes and process optimization [6,66,67]. No general color standards exist for gari, and it depends on the region, country, and whether it is fortified or not [68]. In this study, the creamy yellow color and values reported by Oduro et al., [69], were adopted for comparisons only.

Table 2
Mathematical models fitted to the moisture ratio of the roasting curve of cassava mash (gari).

No.	Types of model	Drying model equation	References
1	Midilli-Kucuk	$MR = aexp(-kt^n) + bt$	[56]
2	Page model	$MR = \exp(-kt^n)$	[57]
3	Lewis model	$MR = \exp(-kt)$	[58]
4	Wang and Singh's model	$MR = 1 + at + bt^2$	[59]

k represents drying constants; *a, b* and *n* are coefficients and *t* is time.

2.8.2. Swelling index (SI)

The SI was determined by filling a 100 ml graduated measuring cylinder to the level of 25 ml with dried gari (V_g) and then topping up the water to the 100 ml marked level. By turning the filled cylinder while securing the top properly upside down, the water and gari were mixed for two minutes. The cylinder was left to stand for 5 min and then the total volume occupied by the mixture (V_f) recorded [39,70–72]. The SI was calculated using the following expression:

$$SI = \frac{V_f}{V_g} \tag{8}$$

2.8.3. Texture

The Henderson and Perry particle size measuring techniques were used in this study. One hundred grams of gari from each run was sieved through a train of graded sieves from 0.5 mm to 5 mm (Fine to coarse grain gari as described by the Codex standards) using the Eijkelkamp VS 1000 shaker set to run for 10 min at 50 Hz [68,73].

2.9. Optimization validation and real-life application procedure

2.9.1. Optimization

The effects of the roasting process parameters (ERP surface temperature and stirring speed) on the final quality of gari (SI, texture and color), roasting time, and energy spent (kWh) were initially selected.

Good gari is considered to swell more than three times in warm water and with texture of between 0.5 and 2 mm [39] and with creamy yellow color [69]. The optimization criteria employed in this work were color comparisons, over 3.0 SI, and minimal energy consumption at minimum texture size. When optimizing processes with many responses, it is recommended to build an appropriate response surface model for each and then determine which operating conditions optimize, replace or keep them within the ranges. Thus, the desirability functions technique (a transition of the response variable from a 0 to 1 scale) was used in the current study by applying Equation (9). Zero and one indicate the completely undesired and highly desirable reactions, respectively [74].

$$D = d_1^{w_1} d_2^{w_2} \cdots d_k^{w_k} \tag{9}$$

where w_1, w_2 and w_k, denote the scale of importance and d_1 to d_k present the number of responses, overall desirability, and individual desirability, respectively.

The importance-based desirability functions of the RSM evaluated in this work were based on specified response goals and importance at (importance, criteria). The response goals and importance were set at (importance, criteria); for time (0.05, minimized), energy (1, minimized), L^* (0.03, match target), b^* (0.03, maximize), a^* (0.03, match target), SI (0.25, maximized) and texture (0.13, minimized).

2.9.2. Real-life application

This study was based on the cassava roasting activities performed in the Maritime region in Togo partially covered in other publications [38]. The dimensions of commonly used roasting pans (wok-shaped) were adopted for possible conversion from woodfuel to solar PV. The next sections highlight the methods taken to complete the PV roasting pan design and performance evaluation utilizing the optimized lab-scale data as a baseline.

2.9.3. Prediction models automation, real-life application and Bland-Altman validation

The optimized coefficients generated from the non-linear robust regression techniques in JMP were automated in python to enable the prediction of design parameters of the real-life roasting pan. A large-scale roasting pan was designed and tested using predicted values thereby generating independent data for external validation [75].

Predictive modeling: A Random Forest Regressor (RFR) model (Script 2) was developed using python and the scikit-learn module to predict the temperature, energetic (SEC, power) and quality performance (color components (L^*, a^* *and* b^*), swelling index, texture and time) metrics based on the optimized temperature and agitation speed. Different researchers have predicted different research parameters using RFR [76,77]. To verify extrapolation reliability, the model's performance was validated using conventional Goodness of Fit (GoF) measures; coefficient of determination (R^2, Root Mean Squared Error (RMSE) and the Mean Absolute Error (MAE). The GoF techniques having been used to verify model performance [78].

In both cases, the model creation were implemented using the sklearn modules and the training was achieved using the independent variables agitation speed and temperature and dependable valuables; time (min), L^*, a^*, b^*, texture (mm) and the swelling index.

Roasting pan geometry and scaling analysis: Using the RFR's parabolic and frustum models, the surface area of the roasting pans were calculated. The dimensions of the big roasting pans typically used for Togo's gari processing were found to be 0.7 X 0.7 X 0.4 m (length, width and depth) made out of cast aluminium.

Energy, power and quality parameters estimation: The predicted energy and quality parameters values for the lab-scale roasting pan were used to calculate the design parameters for the real-life roasting pan for the field application in Lome, Togo. Total energy demands were calculated by taking into account cooking time, roasting pan volume/area ratios, ambient (initial temperatures), and specific heat capacities. The big roasting pan was designed and manufactured based on these predicted parameters (pictorial view in Fig. S2).

External validation and agreement testing: The ESP-WROOM-32 modules were used to manage the voltages, currents and temperature of the developed solar PV powered roasting system (real-life). The application of the ESP-WROOM-32 controller has been explored by others [79,80]. Through the Maximum Power Point Tracking (MPPT), and irradiation temperature, voltage, current (energy) data loggers (Fluke Hydra Data Logger 2620A), the thermal and energetic data were mined. All the cassava mash pre-processing was achieved based on the traditional practices [81]. The samples from each batch were collected and subjected to color, swelling index, texture and other evaluations as highlighted in Section 2.8 and as discussed by [38]. In order to adapt the 40 RPM lab-scale speed, the agitation speed was manually controlled by setting intervals at 40 times per minute.

To validate the prediction models the predicted energy and quality values were compared to the real-life performance evaluation data using the Bland-Altman analysis (Script 3 and 4). This statistical method assesses the agreement between two sets of different measurements and detects any systematic biases or discrepancies and have been applied by other researchers in different fields [82].

The evaluation of the prediction accuracy was further supported by other reliable statistical performance metrics, including the ANOVA, Whitney U test, and Levene's tests (R2, modified R2, RMSE, and MAE), which provided a comprehensive and potent validation of the model's performance on fresh, untested data [83]. The Python scripts and visualizations that were written out (Scripts 1 and 4) automatically incorporated all of these statistical techniques. Multiple comparisons were performed using Tukey Honestly Significant Difference (HSD) tests [84].

Although the data was derived from real-life circumstances, some challenges remain. The models focussed on roasting pan metrics, temperature, time, energy, quality parameters and agitation speed as the main input parameters, with potential influences such as material composition, heat loss to the environment, and operational settings (energy source disruptions) not fully included and calls for further studies. Furthermore, while the random forest gave useful insights, additional research into other machine learning techniques or hybrid models could improve forecast accuracy and generalizability.

Future studies should concentrate on expanding the models to include more operational and environmental parameters, such as fluctuations in solar irradiance and heat loss, material qualities, and AI

integration for smart roasting possibilities.

3. Results and discussion

Appendix A contains the lab-scale results of the experiments carried out in this study. The production yield ranged between 51.33 and 56.67% (0.154 to 0.17 kg). The initial moisture content was found to be 48.6% (0.1458 kg) and 0.1542 kg solids. Results of the performance assessment of the large roasting PV pan are highlighted in Table S1 (supplementary materials)

3.1. Model fitting

The results of the performance of all the terms highlighted in regression equation coefficients Table 3 and the effect summary in Fig. 2 were used to check each coefficient term's significance.

Roasting temperature had a substantial linear effect on all measured response variables, including time, L^*, b^*, and texture ($p < 0.00000$), energy ($p < 0.0079$), SI ($p < 0.00140$), and a^* ($p < 0.00001$).

The linear terms of the roasting agitation speed were significant for time, energy and texture. The above temperature interactions may explain why regardless of magnitude of the stirring speed, the increase in temperature over time resulted in the cassava mash moisture and weight losses. Other researchers have highlighted that as the temperature rises, the physical properties and chemical reactions of the substance being roasted, including moisture content, Maillard reactions, caramalization, and texture, are directly impacted and may be significant in the process predictability [85,86]. Similarly, whether the RPM was less than or greater than 40, particle sizes were larger, roasting was delayed, or more energy was consumed, emphasizing the effect of stirring speed on texture, roasting duration, and energy consumption.

For the temperature, the quadratic terms were significant for the time ($p < 0.00009$), energy ($p < 0.00001$), L^* ($p < 0.00044$), b^*, ($p < 0.00002$), and SI ($p < 0.04108$). The stirring speed quadratic terms were significant for energy ($p < 0.00003$). This suggests that temperature had a higher nonlinear impact on the formation of texture, color, energy, and SI. This concurs with findings from other researchers [5]. The interaction terms of the roasting temperature and the roasting speed had a significant influence on the time ($p < 0.00005$).

The moderate R^2 of 0.56 observed in SI may be related to the limited variability in the values obtained through experimentation, as indicated in Appendix A. Nearly 80% of the values were within 0.7 above the model specification (3.0), while the lowest SI value was only 0.4 away from it. Reduced R^2 is the outcome of minimal data variability in the dependent variables. Nonetheless, the models were deemed to be well-fitting with high F-Test and lower *P-Values* [87].

The R^2 values of 0.56 to 0.96, which show that the models explain 56% to 96% of the variation in the data, are compatible with lower root mean square error (RMSE) of some prediction models, such as the energy model that differed from the experimental data by only 0.10 kWh. These findings imply that the proposed models in this study are appropriate, with no notable lack of fit and strong to moderate R^2 values for all parameters.

Overall, this study highlights how complicated interaction of independent and dependant factors in the roasting processes are. For example, for time, the negative β_1 and β_2 value indicate that as temperature and agitation speed increase the roasting time reduces. Equally, positive interactions witnessed in β_{12}, β_{11} and β_{22} suggests that the effect of one predictor (T or AS) depends on the level of each other, nonlinear relationship between temperature and time and non-linear relationship between agitation speed and time respectively. This means that temperature and agitation speed have non-linear relationship with time.

While the interactions between temperatures and agitation speeds, and the quality parameters investigated in this study were highlighted, there may be other unmeasured variables such as humidity and pressure that could influence the results, potentially confounding the observed interactions. Future research should consider these additional variables.

3.2. Effect of roasting temperature and agitation speed (factors) on evaluation parameters

Fig. 3 depicts the effects of roasting temperature and agitation speed on energy, time, color variables (L^*, a^*, and b^*), texture, and SI using three-dimensional response surface plots.

3.2.1. Effect on energy consumption

The energy and specific energy consumption ranged from 0.16 to 0.76 kWh and 0.68 and 2.79 kWh kg^{-1}, respectively as indicated in Appendix A. Fig. 3(A) shows a three-dimensional response surface plot for energy as a function of roasting factors.

As highlighted in Fig. 3(A), the quadratic and linear terms of the temperature, and the linear coefficients of the stirring speed are the most significant on the specific energy consumption. This interaction could be the reason why it was observed that at certain temperatures and stirring speed interactions, the energy consumption varied significantly. This agrees with the results highlighted in Appendix A and Fig. 3(A), where at lower agitation speeds (10 to 20 RPM), the energy consumption was high as the temperature increased. However, as the stirring speed ascended from 20 RPM, the energy consumption decreased before increasing again at speeds above 40 RPM demonstrating the quadratic relationships. The physiochemical property changes occur more quickly at higher roasting temperatures; however there may be a trade-off between increased energy demand and increased energy consumption at higher temperatures. agitation speed can also impact the uniformity of heat transfer and the rate of water evaporation which is difficult to attain at lower stirring speeds and higher temperatures [88]. The most and least energy consumptions of 0.76 and 0.16 kWh were achieved at 130 °C (10 RPM for 34 min) and 90 °C (40 RPM for 29 min). The run with the lowest energy consumption did not satisfy the quality requirements of swelling three times, just like the moderate energy-consuming runs at higher temperatures that resulted in higher texture (above 5 mm) due to lamping. This could demonstrate that temperature and stirring speed play important roles in the effectiveness and quality of the roasting process and their effects on the energy consumption and

Table 3
Regression equation coefficients for roasted cassava gari, shown as actual terms and statistical analysis.

Response (Y_i)	β_0	β_1	β_2	β_{12}	β_{11}	β_{22}	R^2	RMSE	P-values	F-Test
Time (min)	17.76	−11.62	−4.85	5.55	7.61	2.43	0.96	2.17	0.0001	169.47
SEC (kWh kg^{-1})	1.74	0.43	−0.30	0.13	−0.61	0.75	0.90	0.19	0.0001	16.77
L^* (−)	70.08	−6.46	0.39	−0.17	5.34	−1.32	0.88	2.02	0.0001	49.51
a^* (−)	−1.38	2.51	−0.21	−0.17	−0.13	−0.93	0.69	1.33	0.0001	15.66
b^* (−)	26.33	2.86	−8.95E-6	−0.61	−3.68	−0.61	0.85	1.11	0.0001	40.71
SI (−)	3.76	0.39	−0.19	−0.17	−0.43	−0.06	0.56	0.33	0.0001	13.96
Texture (mm)	2.33	1.81	−0.50	−0.43	0.42	−0.15	0.88	0.58	0.0001	81.10

β_0 = intercept, $\beta_1 and \beta_2$ = temperature and stirring speed terms respectively (linear coefficients), β_{22} and β_{11} = stirring speed to stirring speed and temperature to temperature interactions respectively (quadratic coefficients), and β_{12} = temperature to stirring speed interaction (interaction coefficients) and SI = swelling index.

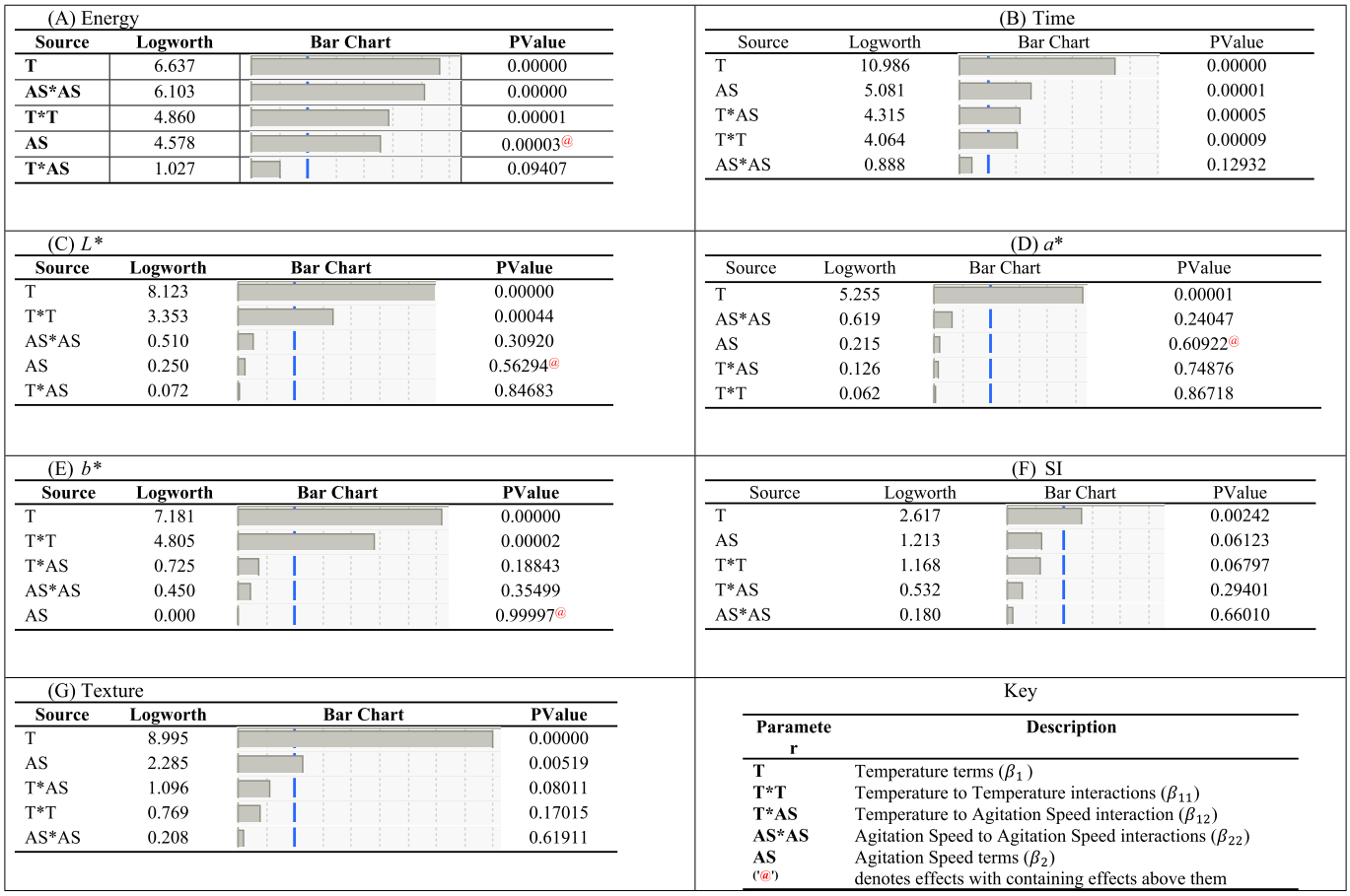

(A) Energy

Source	Logworth	Bar Chart	PValue
T	6.637		0.00000
AS*AS	6.103		0.00000
T*T	4.860		0.00001
AS	4.578		0.00003@
T*AS	1.027		0.09407

(B) Time

Source	Logworth	Bar Chart	PValue
T	10.986		0.00000
AS	5.081		0.00001
T*AS	4.315		0.00005
T*T	4.064		0.00009
AS*AS	0.888		0.12932

(C) L^*

Source	Logworth	Bar Chart	PValue
T	8.123		0.00000
T*T	3.353		0.00044
AS*AS	0.510		0.30920
AS	0.250		0.56294@
T*AS	0.072		0.84683

(D) a^*

Source	Logworth	Bar Chart	PValue
T	5.255		0.00001
AS*AS	0.619		0.24047
AS	0.215		0.60922@
T*AS	0.126		0.74876
T*T	0.062		0.86718

(E) b^*

Source	Logworth	Bar Chart	PValue
T	7.181		0.00000
T*T	4.805		0.00002
T*AS	0.725		0.18843
AS*AS	0.450		0.35499
AS	0.000		0.99997@

(F) SI

Source	Logworth	Bar Chart	PValue
T	2.617		0.00242
AS	1.213		0.06123
T*T	1.168		0.06797
T*AS	0.532		0.29401
AS*AS	0.180		0.66010

(G) Texture

Source	Logworth	Bar Chart	PValue
T	8.995		0.00000
AS	2.285		0.00519
T*AS	1.096		0.08011
T*T	0.769		0.17015
AS*AS	0.208		0.61911

Key

Parameter	Description
T	Temperature terms (β_1)
T*T	Temperature to Temperature interactions (β_{11})
T*AS	Temperature to Agitation Speed interaction (β_{12})
AS*AS	Agitation Speed to Agitation Speed interactions (β_{22})
AS	Agitation Speed terms (β_2)
('@')	denotes effects with containing effects above them

Fig. 2. Effect summary; energy (A), time (B), L^* (C), a^* (D), b^* (E), SI (F) and texture (G) (Values above the blue reference line at 2 are significant at $0.01(\log_{10}) = 2$).

quality parameters during cassava roasting are complex. The findings are consistent with cocoa roasting, where it was found that flavor compounds formed more quickly at higher temperatures initially but that this led to a decrease in their concentration. This emphasizes the significance of process optimization to strike a balance between flavor and concentration [88]. It has also been found elsewhere that the pace at which the palm date seeds are roasted affects the rate of heat transmission and distribution, which in turn affects the hardness, moisture content, and color parameters of the seeds—all of which are connected to energy consumption [89].

The SI and texture of the roasted cassava pulp were found to be within the necessary limits in this study at lower temperatures and moderate stirring speeds, supporting the findings of other researchers that lower roasting temperatures can reduce energy consumption while preserving the desired quality effects [90]. This study further demonstrated that optimizing both temperature and stirring speed is critical to producing an energy-efficient roasting process that achieves the desired quality criteria. It is a delicate balance that must be carefully considered based on the qualities of the specific food, available energy sources, type of roasting model (contact, conviction or direct roasting) and the desired outcome of the roasting process.

The correlation between energy consumption and qualitative characteristics of gari (texture, swelling index, and color components (L^*, a^*, b^*) were investigated and displayed as correlation probability and scatterplot matrix in Appendix C (A) and C (B) respectively. Low *P-values* (less than $p=0.05$) were achieved suggesting a statistically significant correlation. Aside from the degree of whiteness (L^*), which decreased with increasing energy (negative correlation), the green–red (a^*) and the blue-yellow (b^*) opponents had a direct proportional relationship with energy consumption. This could explain why some runs at higher temperatures produced more creamy gari during the experiments, and it might be linked to the pyrodextrinization process, whose rate is higher at higher energy/temperature input [67,89].

The overall energy efficiency ranged between 12.02 and 60.22% as shown in Appendix E. The most energy-effective run never led to the most optimal, as was commonly noticed. This circumstance may be explained by Pareto inefficiency or suboptimality, which occurs when a run or solution falls short of fully satisfying all constraints and objectives or reaches the maximum value of the objective function. In this investigation, the optimal condition was reached when all quality and thermal parameters were satisfied using approaches for desirability optimization [91,92]. Appendix E highlights the energy efficiency ranking in relationship with the temperature, energy consumed, stirring speed, set and final temperatures. The mean energy efficiency was 35.72%. The energy efficiency range achieved in this study is in line with other publications [91,93,94].

3.2.2. *Effect on roasting time*

Fig. 3(B) demonstrated that the roasting process exhibited a negative correlation (roasting time decreased with rising temperatures). While β_1, β_2, β_{11}, β_{12} and β_{22} had significant effects on the roasting duration, the linear terms of the temperature and the stirring speed had the most significant effects as shown in Fig. 3(B). There were nearly equal significant Logworth values for the temperature-to-stirring speed interaction and the temperature-to-temperature interactions (quadratic coefficients). The linkages and interactions between these elements demonstrate the complexity of the roasting process. Appendix A displays the range of roasting times from 13 min (250 °C/30 RPM) to 56 min (90 °C/10 RPM). Generally, the shortest roasting periods witnessed at stirring rates between 20 and 40 RPM. Quick stirring at a specific

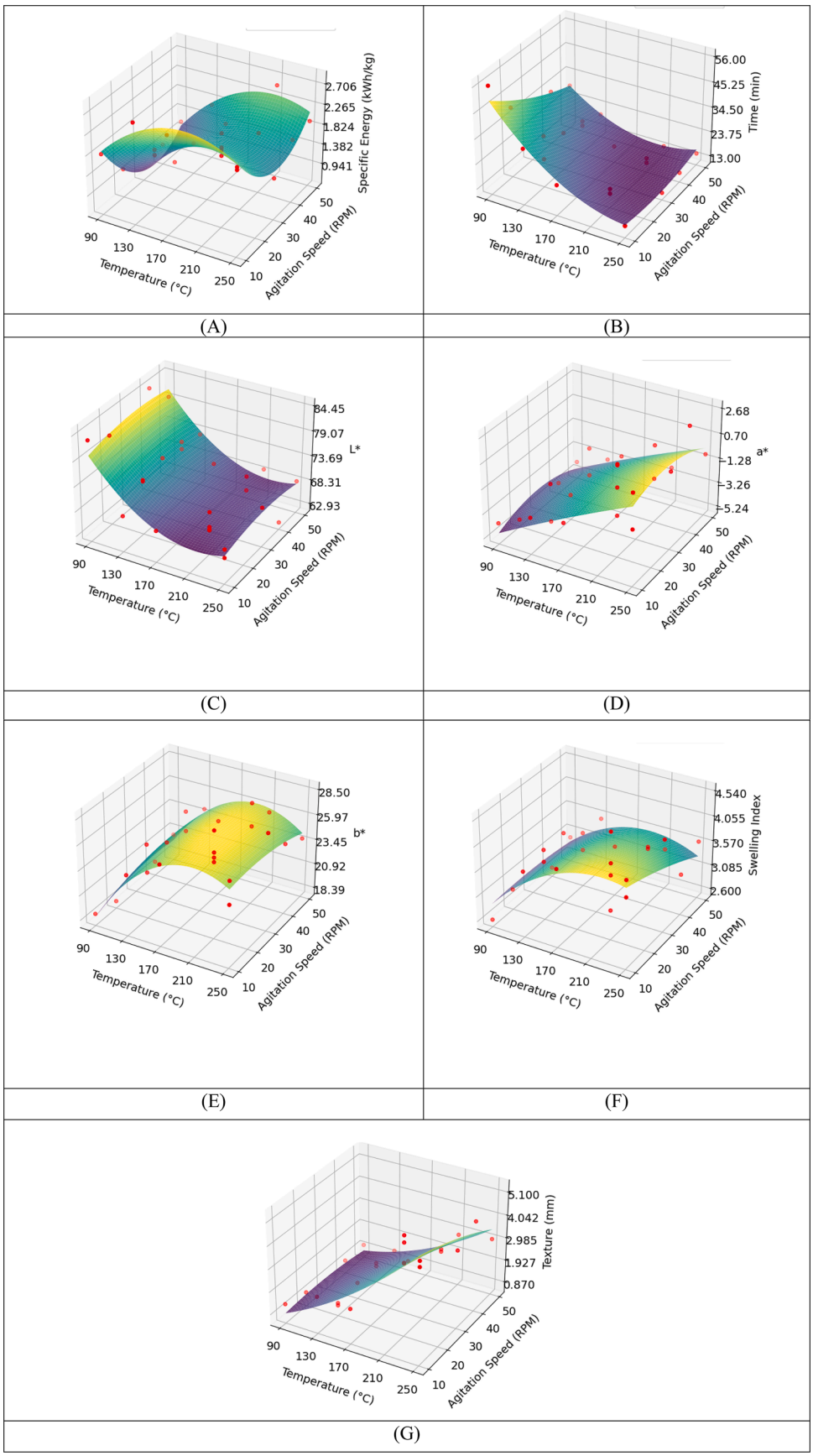

Fig. 3. Response surfaces plots; (A) energy, (B) time, (C) L^*, (D) a^*, (E) b^*, (F) SI and (G) texture.

temperature improves heat transfer performance and hence mass transfer while raising the temperature raises the rate of evaporation [95,96]. Slower stirring speed may result in poor heat distribution, causing some sections of the material to get extreme or insufficient heat, potentially resulting in an uneven roast and burning. Moisture migration may, therefore, slow down, resulting in longer roasting times to achieve the appropriate roast quality. However, excessive stirring may result in greater heat losses and poor heat distribution, resulting in a longer and more uneven roasting process, increased energy consumption, and changes in physical and chemical reactions [97–100]. But how excessive or moderate is the roasting temperature and stirring speed? Optimization of the two factors, therefore, cannot be overstated.

3.2.3. Effect on color

The changes in the color attributes are highlighted in Fig. 3(C, D and E). The temperature linear coefficients had the most significant effect on all the color components even though the L^* and b^* showed stronger temperature quadratic relationships as shown in Fig. 3(C, D and E). It was observed that the L^* values reduced. In contrast the a^* and b^* values increased with the increasing roasting temperatures, confirming the observed situation during roasting where some runs at higher temperatures produced charred clumps of gari. Even if the linear coefficients of the stirring speed were insignificant for the color components (Fig. 3 C, D, E), they statistically denoted effects with containing effects above them. This means that the model heredity identifies the stirring speed as a very critical parameter in color changes during the roasting process and conforming to the effect heredity technique [101]. The higher the temperatures, the lower the L^* values in most of the food products [67]. This could be attributed to the browning and Maillard reactions, and pyrodextrinization processes that are related to higher temperatures above 150 to 250 °C [85,89,102]. It was generally observed that a combination of higher stirring speeds and higher temperatures resulted in a more creamy yellow color output than the combination of higher temperatures and lower stirring speeds that resulted in chard clumps. This could be attributed to the fact that at higher agitation, the heat distribution and mass flow rate are more efficient [103]. Even if the codex standard does not specify the color, researchers have highlighted that a good gari quality should be creamy yellow [68,69]. The creamy yellow color outputs *(b^*)* attained in this study are within the recommended band of 19.96 to 43.22 [69]. In this study, moderate a^* and b^* values were obtained between 30 and 40 RPM; nevertheless, the higher the stirring speed, the higher the L^* values. Managing temperature and stirring speed is essential to achieving the desired color values and changes that are key to food quality and process conditions optimization [6,89].

3.2.4. Effect on the texture and SI

During roasting at temperatures above 170 °C, larger particle sizes (above two mm) were observed as confirmed in Appendix A and Fig. 3 (G). The swelling index was greatly affected by the linear and quadratic temperature coefficients, while the texture was affected by the linear terms of the temperature and the stirring speed as shown in Fig. 3(f and g respectively). This means that the temperature had a greater effect on the swelling index and at different temperatures, different swelling indexes were observed. However, the combination of the stirring speed and temperature effects, moderately affected the particle sizes (texture). The runs from 210 to 250 °C resulted in higher particle sizes above three mm and agglomeration was observed in runs operated at 250 °C with 10 RPM. It was, however, observed that the run with 50 RPM at 250 °C resulted in a much finer texture. Naturally, starch is sticky, and its rate of gelatinization is faster at higher temperatures and enough moisture content [104,105]. It is possible to deduce that higher stirring speed causes quicker evaporation, preventing particles from sticking together and resulting in finer texture. Higher stirring speeds guarantee equal heat distribution, which could prevent starch particles from sticking to the hot roasting pan surface. Texture is roasting process parameters specific [106].

As seen in Fig. 3 (F), the higher the roasting temperatures, the higher the SI values obtained in these investigations. Denaturation of proteins, the gelatinization of starch, and the heat's impact on food's cell wall structures that result in solubilization by fibrous structure puncturing, have a substantial impact on the swelling index (SI), and the perfect pace of stirring is crucial for optimal quality SI [5]. The temperature greatly influenced on the texture and SI of the roasted cassava mash to gari.

3.3. Optimization

Heat is used for stimulating starch gelatinization in the roasting process of foods such as cassava into gari. This occurs when moisture content, stirring speed, and temperature interact. Optimized roasting conditions can lead to faster water evaporation, energy savings, and a higher quality end food product. Therefore, optimization of the important parameters is critical. In Fig. 4 the desirability function response surface optimization technique used in this study is illustrated. The roasting temperature of 130 °C at 40 RPM stirring speed was found to be optimum at a desirability of 0.99. At these factors, the optimum responses were; time (22.27 min), SEC at 1.37 kWh kg^{-1}), L^* (74.55), a^* (−2.97), b^* (23.98), SI (3.40), and texture (1.36 mm).

This study has demonstrated that roasting is a complex process because changes to one parameter may impact others, ultimately affecting the quality of the final product. Additionally, it was observed that at both lower and higher roasting temperatures and stirring rates, a non-uniform textural profile was obtained that corresponded to a non-uniform temperature distribution throughout the sample. To balance the conflicting responses in the roasting processes, trade-offs in factors must be made rather than aiming for the highest or least values of all responses [6,107].

Understanding the fundamental interactions of temperatures (heat distribution), stirring speed, mass transfer, and their optimal points in roasting may make it easier to modify old approaches (traditional) and produce more successful innovations. This could help to preserve quality and sensory features thereby increasing the acceptability of new sustainable solutions [108].

The optimized run was further subjected to other analysis such as the validation and real-life applications, drying kinetics models fitting, *RoR* analysis and energy distribution as discussed in the following sections.

3.4. Validation and real-life application of models

3.4.1. Validation of predictive models using goodness of fit metrics

With R^2, RMSE and MAE values ranging from 0.56 to 0.94, 0.32 to 2.44 and 0.12 to 1.56 respectively across the dependent effects as shown in Table 4 (Script 1), the models demonstrated high predictive ability accounting for 56–94% of the variance in the experimental data (lab-scale). All responses had the adjusted R^2 values above 0.80 apart from the swelling index (0.41) and the a^* (0.58). Lower R^2 and adjustable R^2 for the swelling index and the a^* could be attributed to the limited variations in response variables across experimental conditions witnessed in this study. For example, all the runs apart from those that operated at 90 °C resulted into the swelling index above 3.0. It has been highlighted by other researchers that a low adjusted R^2 does not necessarily result into a bad model, but could indicate that the effect been investigated does not significantly change under the experimental conditions because the model has little explanatory power [109].

The high prediction accuracy of the models highlights their significance in optimizing process parameters. For example the models of the time, specific energy consumption and L^* with R^2 of 0.94, 0.90 and 0.85 respectively, provides reliable tools for determining ideal conditions to achieve the desired product quantity, quality and with visual satisfaction while minimizing energy consumption.

Despite the' strong overall performance of the models, the *RMSE/MAE* ratio for the time exceeded 1.5, which may be explained by the

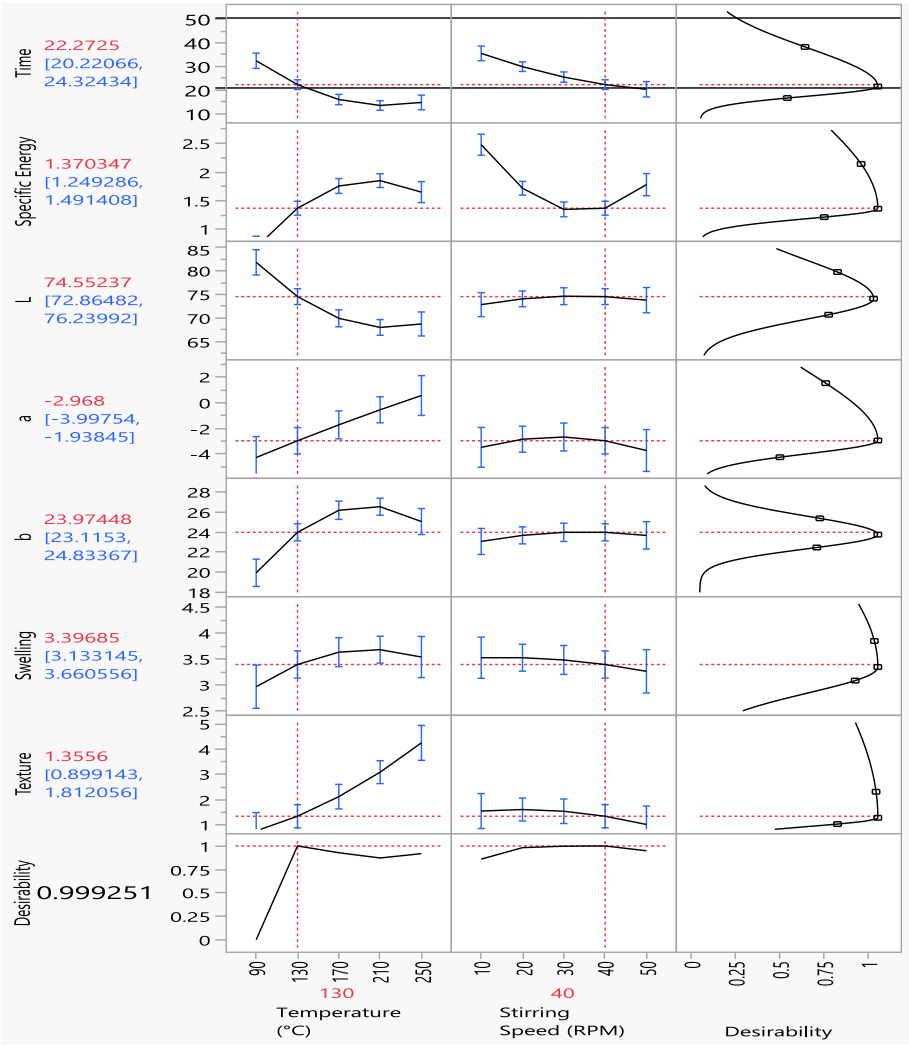

Fig. 4. Prediction profiler for the cassava roasting process parameters optimization.

Table 4
Validation matrix for the prediction models.

Parameter	R^2	Adjusted R^2	RMSE	MAE	RMSE/MAE
Time	0.94	0.92	2.43	1.57	1.55
Specific energy	0.90	0.86	0.17	0.14	1.21
Texture	0.88	0.85	0.50	0.39	1.28
Swelling index	0.56	0.41	0.32	0.25	1.28
L^*	0.85	0.80	2.02	1.49	1.36
a*	0.69	0.58	1.23	1.07	1.50
b*	0.85	0.80	1.03	0.90	1.44

time-dependent processes' intrinsic nonlinearity and variability which the current model may not fully account for. According to Ali et al, [110], ratios greater than 1.5 are linked to either excessive variability in variable patterns or a model that is too simple to account for non-linear connections. Future research could involve incorporating additional predictors or using other non-linear modeling approaches to better capture the dynamics of time dependent responses.

After having met the basic validation matrixes, the models were applied to larger-scale operations using machining learning (random forest), and the performance evaluation is detailed in the section that follows.

3.4.2. Real-life application: Designing and analysing of scaled predictions (quality and energy metrics)

The Random Forest models (Script 2) accurately predicted the operational parameters for the most commonly used roasting pan size in Togo for cassava roasting using the lab-scale optimized and validated predictive models, as illustrated in Fig. 5 (a). The design parameters were: SEC = 1.68 kWh kg-gari^{-1}, time = 23 min, L^* = 73.44, a^* = −2.50, b^* = 24.57, swelling index = 3.55 and texture = 1.12 mm.

The surface volume and mass ratios of the lab-scale to real-life roasting pans ranged from 1 to 7 (0.028 to 0.1969 m^2) and 1 to 4.5 (4.5 to 20 kg) respectively. The greater surface area enhances heat transfer, but it may also result in excessive energy consumption due to the roasting pan's larger mass [111]. To reduce the heat loss, the outside insulation of the roasting pan was reinforced.

Changes in the ambient temperature had a substantial impact on the energy required for roasting with a factor of 2 (40 to 20 °C, lab-scale to real-life). Increased initial temperatures resulted into the reduction of the temperature differential (ΔT) between the targeted temperature of 130 °C. This reduction led to lower energy demands for heating the substance and the roasting pan. The random Forest model factored in this energy load factor emphasizing its reliability in various ambient conditions. These findings highlight the importance of considering ambient conditions in energy systems designing and assessment for the roasting processes [112].

Even if the design process was well executed, future studies should

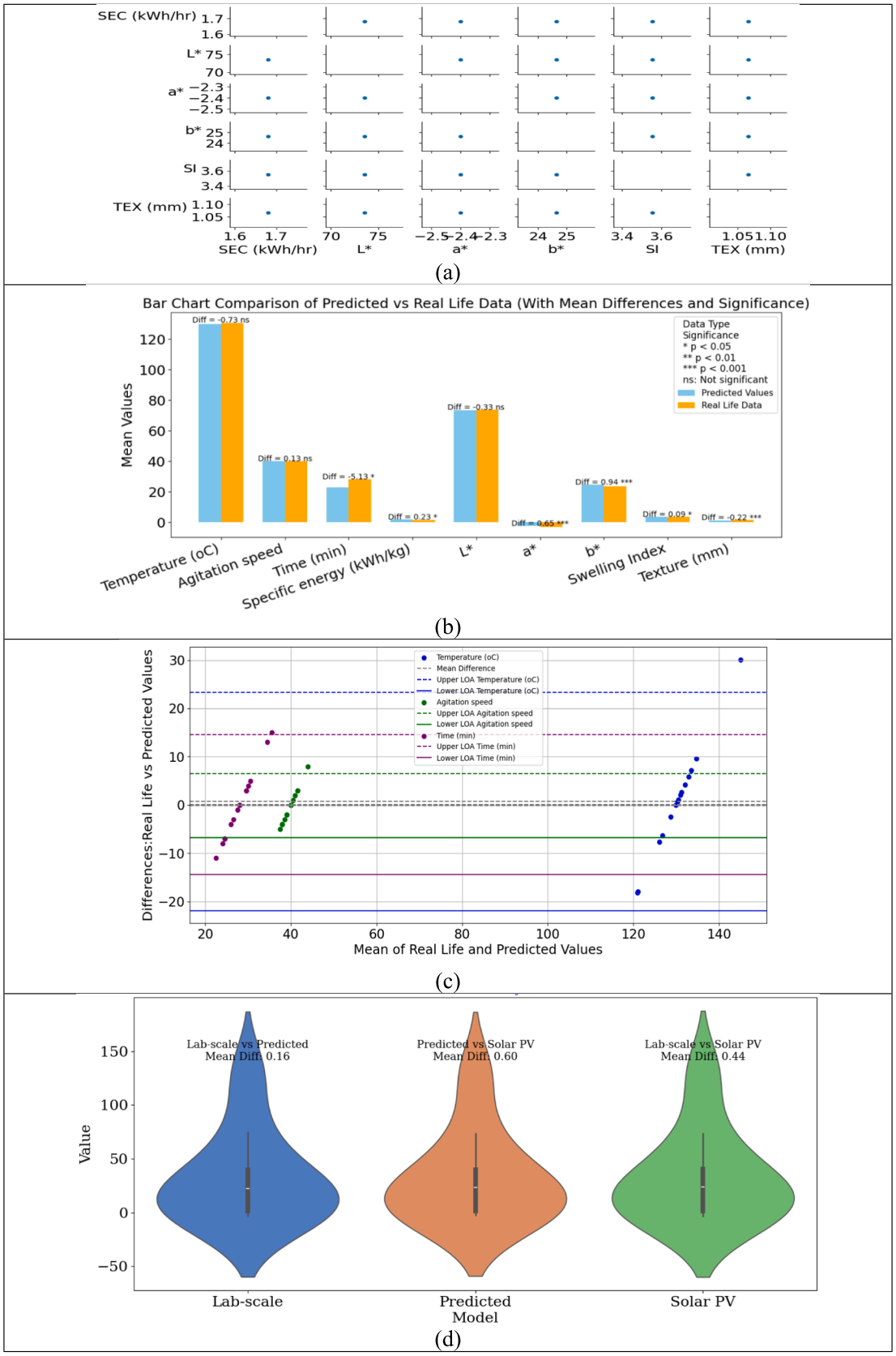

Fig. 5. Comprehensive analysis of predicted vs real-life data; (a). Designing and analyzing scaled predictions: quality and energy metrics, (b). Bar chart comparison of predicted vs. real-life data with mean differences and significance, (c). Bland-Altman plots for predicted vs.real-Life Data (SEC = Specific Energy Consumption, SI = Swelling Index, TEX = Texture, Diff = mean difference and (d). Violin plot of models values with Tukey Honestly Significant Difference (HSD) mean differences (Solar PV = real-life application).

explore the use of more advanced machine learning models such as neural networks and ensemble learning to enhance the accuracy of predictions for energy and quality parameters. These models could also incorporate additional features such as humidity and specific roasting pan coatings.

The roasting pan was developed and set up at Lome University in Togo. Table S1 highlights the performance evaluation, while the following section discusses the predictive models and real-world comparison outcomes.

3.4.3. Comprehensive analysis of predicted vs real-life data (validation)

The major purpose of this investigation was to determine how effectively the prediction model generated from the lab-scale system replicates real-world outcomes across a variety of factors, including temperature, agitation speed, and specific energy.

The mean difference bar chart Fig. 5 (b) illustrates the differences between expected and actual means for each effect (Script 4). Overall, the model exhibited negligible mean differences for the majority of impacts, indicating a strong fit with real-world data. For example, the mean difference for temperature was just 0.73 °C which was not significant different from the 130 °C prediction, indicating accurate forecasts. However, the model somewhat overstated texture ($p < 0.001$), a^* ($p < 0.05$), and specific energy ($p < 0.05$), values, which may have an impact on the particle sizes, the color and energy efficiency forecasts. It was nice, however, to get a better texture for the gari than expected.

Differences in texture could be attributed to differences in grating equipment, roasting operator expertise, or heat application moods [113].

The Bland-Altman plots, which are summarized in Fig. 5 (c) and separately for the factors and effects shown in supplementary materials (Fig. S3) performed in Script 3, allowed for a deeper comprehension of the agreement between predicted and actual values. At −5.13 min, time had the smallest negative mean difference, whereas b^* had the largest positive at 0.94 (average bias).The positive sign signified that the predicted value was higher than the real-life, e.g. predicted time was 23 min while real-life was 28.1 min. Close alignment on averages of the real-life values and the projected between the temperature agitation speed and L^*, was observed with a not significant affirmation as shown in Fig. 5 (b).

However, the standard deviations of 11.52 and 0.04 (higher or below ±1.93) for temperature and texture, respectively, indicate that, while the average forecasts were close, individual batch estimates varied significantly. This is demonstrated by the disparities between the predicted 23 min and the 28.1 min real-life roasting time. The higher time difference could be as the result of the solar irradiance swings that greatly affected the temperatures.

In Fig. 5 (d), the optimized lab-scale, RF predicted and the real-life (Solar-PV) mean values are compared. The results of the Tukey HSD test indicate that there are no statistically significant differences between the models means specifically with a p-value of 1. This means that any observed differences are consistent with random variation, implying that the models performed similarly in terms of the measured parameters [84].

This also explains the variety in individual batch variables, such as temperature, where the lowest was 111.91 and the highest was 160.08 °C, as shown in supplementary materials Table S1. The results show that, while the model performed well overall and all the effects kept within the standard and quality requirements, aspects such as temperature, texture, and specific energy that might fall under or higher the target of ±1.91 set by the Bland-Altman (130 °C, 40 RPM and 26 min), require additional study techniques to improve practical dependability as recommended by [114]. The main cause of the fluctuation could be attributed to rapid variations in solar PV irradiance. This begs for more studies on how to combine the inconsistencies that come along with the energy sources, quality of raw materials (cassava), human interface, climate circumstances, and technology used during model and design forecasts.

The predicted values are close to the real-life averages, which are encouraging and indicative of a strong agreement on a general level. Even if the Bland-Altman analysis indicated that there is significant variability in individual batch forecasts, as seen during the evaluation of the PV-powered roasting system, other studies have recommended that so long majority data points fall in between the upper and lower LOA (as a case in this study Figs. S3), the reproducibility and credibility of the results is good [115,116].

A rigorous comparison undertaken between the electric energy powered roasting systems (Lab-scale, predicted and solar PV-real-life) and the woodfuel cookstoves currently been used in the Maritime region in Togo. The results as reported in Table 5, show significant energy savings of around 81.41% with electric powered devices. The higher temperatures recorded in contrast to the optimized 130 °C achieved by the electric energy-powered roasting equipment could illustrate the inefficiency of traditional woodfuel cookstoves [16]. These findings demonstrate the potential for significant energy savings and efficiency advantages through the implementation of improved roasting technology.

3.5. Roasting kinetics and energy distribution of the optimized run (130 °C, 40 RPM)

3.5.1. Temperature profiles, RoR and RoEv

The highest *RoR* of roughly 21.08 °C min-1 (0.35 °C second^{-1}) was attained in minute 2.23, which corresponded to temperatures of 71.50 and 133.20 °C for the cassava mash and roasting pan surface, respectively, as shown in Fig. 6. Consequently, the moisture content of the cassava mash decreased steadily from 0.95 to 0.87 dry basis as the temperature increased as, shown in Fig. 7 from S_2 to S_3 translating into 0.012 kg cumulative evaporated water at V (0.004 kg min^{-1} *RoEv*). This stage could have portrayed the initial adjustment period of drying where the pre-heating takes place as indicated in Fig. 7 (S_0 to S_2) and lasted for only one minute [117]. It might be concluded that the initial drying period coincided with the constant rate period.. This is in agreement with the observations from other researchers who deduced that the surface water and the interstitial water get evaporated initially followed by the free water in the constant rate period [118,119]. The RoEv curve was stepper in the first 4 min (S to A) of the process than the rest of the process (A to C), further indicating that the dehydration rate was faster from S to A as than from A to D.

As the temperature of the pulverized cassava mash increased from A_1 to A_3 via A_2, it could be seen in Fig. 6 that the *RoR* was turbulent (from A_1 to B_1). There are several possible causes for the instability in the *RoR*, including thermal inertia from the initial quick heat absorption of the cassava mash particles, which could result in a dramatic increase [120,121]. Generally, unstable heat distribution could result in unstable heat transfer to the cassava mash surface [122].

Between minutes 3 and 8, the *RoR* stabilized and subsequently

Table 5
Comparison of the lab-scale, predicted, solar PV (real-life) and the woodfuel cookstoves values.

Parameter	Lab-scale	Predicted	Solar PV	Woodfuel cookstoves
Temperature (°C)	130	130	130.73	494.28
Agitation speed (RPM)	40	40	40.2	N/A
Time (min)	22.27	23.59	28.13	20.86
Specific Energy (kWhkg^{-1})	1.37	1.68	1.45	7.37
L^*	74.55	73.44	73.67	73.96
a^*	−2.97	−2.5	−3.15	−3.25
b^*	23.98	24.57	23.63	24.48
Swelling Index	3.41	3.55	3.41	3.85
Texture (mm)	1.36	1.12	1.34	1.69

Woodfuel cookstoves data from [16].

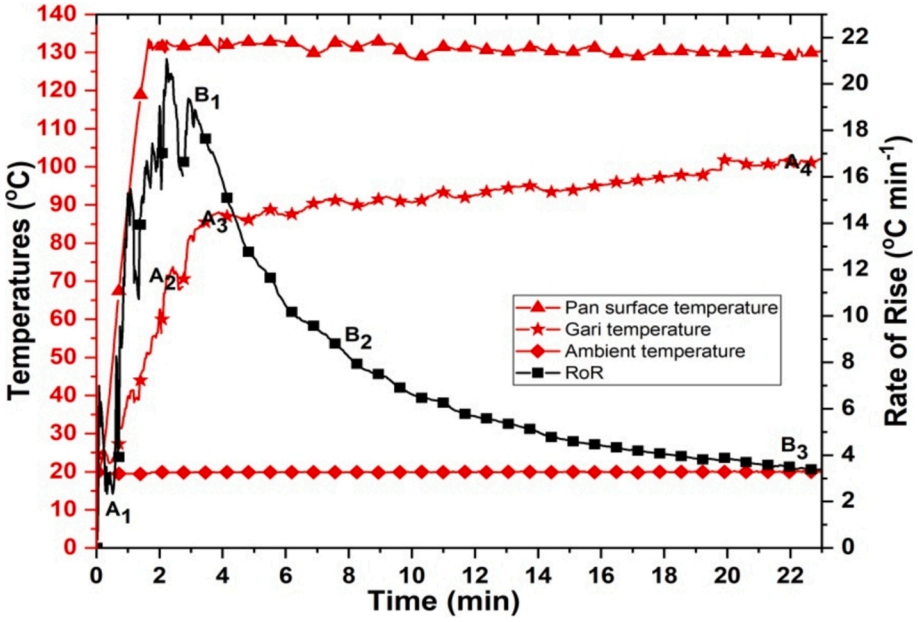

Fig. 6. Roasting process dynamics: temperature profiles and Rate of Rise vs. time.

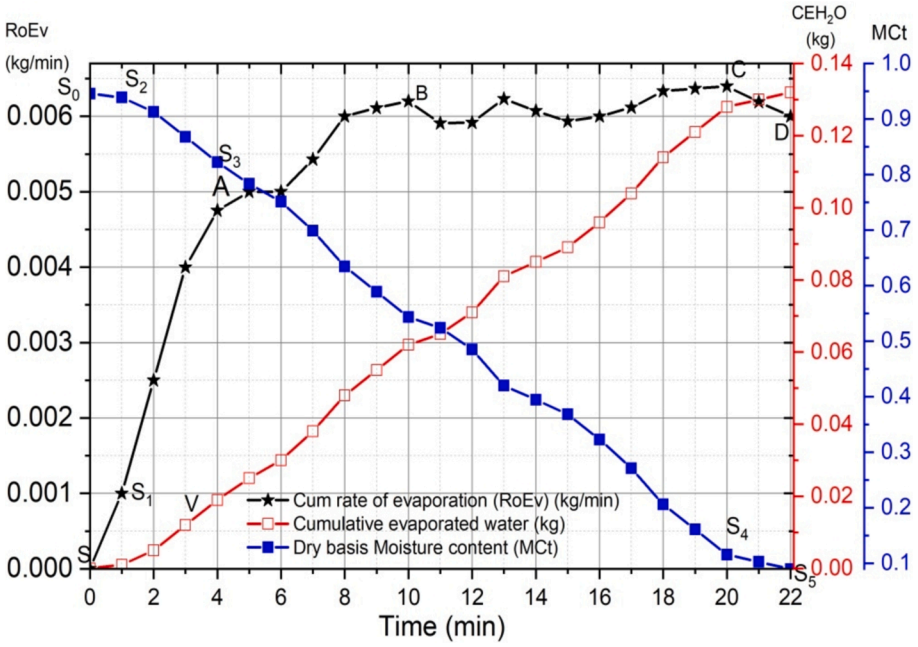

Fig. 7. Dynamics of moisture content and water evaporation during roasting over time.

declined from approximately 19.20 to 7.97 °C min^{-1} (Fig. 6). The stability could be explained by the roasting pan surface temperatures remaining stable at around 130 °C, resulting in a gradual increase in cassava mash temperature from around 85 to around 101 °C by the end of the roasting process. Smooth temperature changes in the product being roasted result in smooth *RoR* [31]. This time frame might represent the first falling period (S3 to S4 Fig. 7). After 15 min of processing, the color of the cassava mash started changing from white to creamy white. This may be attributed to the fact that starch granules, when heated in the presence of water, absorb water and swell, making it easy for some starch components, mainly in the form of amylose, to leach out of the granules and solubilize. The granules rupture (gelatinize) when the temperature and the water absorption increase [123].The presence of moisture and cassava mash temperatures above 80 °C during this time frame may have allowed gelatinization of starch and detoxification [106,124,125].

The second falling stage lasted from minute 20 to 22 (end of the roasting procedure), by which time the cassava mash had converted into gari (S4 to S5 in Fig. 7). When the temperature of the cassava mash exceeded 94 °C (minute 15) texture creation became obvious, but the moisture content remained high. However, in minute 22, the moisture content was reduced to around 10.2%, and the degree of dryness was sufficient to affect the gari's crispiness. The total cumulative water evaporated was 0.132 kg. The achieved temperatures were significant to affect the quality (color, sensory, and swelling index) of gari. Furthermore, the duration attained of 22.27 min is lower than the 30 min reported by other researchers [126]. The differences might be due to the different cookstoves and energy sources.

3.5.2. Energy consumption and energy efficiency

Fig. 8 illustrates the energy performance. Fig. 8A displays the specific energy consumption (SEC) and Cumulative Specific Energy Consumption (CSEC) in kWh kg^{-1}, whereas Fig. 8B displays the energy consumption and Cumulative Energy Consumption (CEC) in kWh. In the first two minutes of roasting, peak energy consumption and SEC were 0.022 kWh and 0.076 kWh kg-1, respectively, generating 0.18 kW CEC and 1.14 kWh kg^{-1} CSEC. The energy consumption remained stable between 0.09 and 0.01 kWh (0.029 and 0.04 kWh kg^{-1} SEC) until the roasting process was completed. The first peak, which is also shown in the temperature graph (Fig. 6), may be related to the energy required to start the cooking process and overcome the thermal inertia of the cassava mash and cooking utensils [90]. The total energy efficiency of this run was 54.93%.

3.5.3. Drying kinetic modeling

Generally, the roasting of cassava mash to gari showed similar drying characteristics to most agricultural products, as indicated in Fig. 9. The Midilli-Kicuk model was preferred even though it had a lower R^2 (0.9974) than the Page model (0.9982), as shown in supplementary matterials (Appendix D). This is because the difference in R^2 (0.08%) is very small, but the SSE (0.00537 for the Midilli-Kicuk and 0.0156 for the Page) is significantly different by 65%. As demonstrated in Table 3, the Midilli-Kucuk's lower SSE, MSE, and RMSE suggested a better overall fit in terms of error minimization. A lower SSE suggests a better match [6,29,54]. Table 6 shows the values for the four constants (a, b, k, and n) in the equation that defines the Midilli-Kucuk model.

In terms of drying time at selected temperatures for roasted cassava mash into gari, the difference between the experimental and predicted MR using the most suitable models is displayed in Fig. 9. The models used in this study (Table 6 and Fig. 9) satisfactorily demonstrate to represent the drying characteristics of cassava mash to gari, although the experimental roasting time did not exactly match the actual data. This situation has been reported by other researchers [127–130]. To explain the drying behavior of various materials, including groundnuts [131], bay leaves [132], apricot kernels [133], moringa leaves [28], and many more numerous researchers have also fitted the Midilli-Kucuk kinetic as the best thin layer drying model to their data [134,135].

Therefore, by optimizing the Midilli-Kucuk drying kinetic model for the roasting of cassava mash at 130 °C and 40 RPM stirring speed in this study, the most appropriate thin layer equation proposed could be defined as:

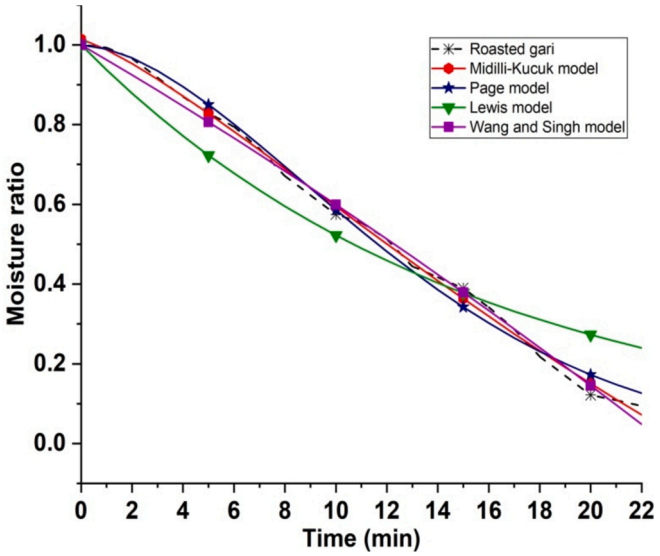

Fig. 9. Fitted drying kinetics for the optimized cassava mash to gari run (130 °C and 40 RPM).

$$\boldsymbol{MR} = 1.0143\mathbf{exp}(-0.01255\boldsymbol{t}^{1.4038}) - 0.01434\boldsymbol{t} \quad (10)$$

As depicted in Equation (10), the coefficient of the constant '*a*' represents the material's initial moisture content. According to certain researchers, optimizing the *"k"* constant has a significant impact on the dying system's energy efficiency [56,136–138]. When investigating the behavior of the drying kinetics of drying *Moringa oleifera* at different pretreatment statuses, Ambawat et al. [28] observed an increase in '*k*' and '*a*' coefficients as the temperature increased. This led them to postulate that the product's internal diffusion mechanism and the environment's capacity to absorb the water could cause an acceleration of moisture migration in response to temperature increases. Coincidently,

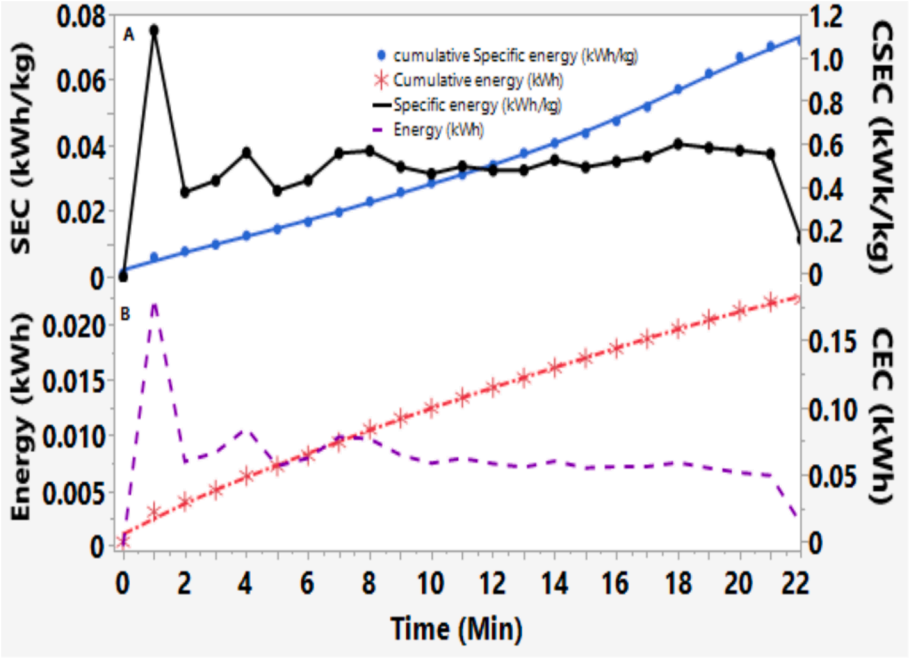

Fig. 8. Roasting process energy performance of the optimized run.

Table 6
Parameters of the drying models and goodness of fit achieved for the cassava pulp roasting.

Model	SSE	MSE	RMSE	Constants			
				k	*n*	*a*	*b*
Midilli-Kucuk	0.00537	0.000283	0.01681	0.01255	1.4038	1.0143	−0.01434
Wang and Singh	0.011587	0.000552	0.02349	–	–	−0.03744	−0.00026
Page	0.015573	0.000742	0.02723	0.01026	1.7168	–	–
Lewis	0.176605	0.008028	0.08960	0.06491	–	–	–

k represents drying constants; *a, b* and *n* are coefficients and *t* is time.

this study found that the drying curve grew steeper at higher roasting temperatures, a strong signal for higher drying rates, as Fig. 5 (A_1 to A_3), 6 (S to A), and S_2 to S_4 illustrate. As a result, as the temperature increased rapidly, the *RoR* became unstable, as shown in Fig. 6 (A_1 to B_1), and energy consumption increased (Fig. 8).

The model achieved in this work exhibits nonlinearity and an accelerated first falling drying phase behavior, which is further confirmed by the positive '*n*' constant greater than 1. It was physically observed that most of the weight in the cassava mash, which signified moisture loss (drying), was achieved in the first drying period, with temperatures ranging from 88 °C to 101 °C for the cassava pulp and an average of 130 °C for the roasting pan surface. After heating, free moisture in the material evaporates from the solid surface. The higher the temperature of the roasting pan, the higher the temperature of the cassava mash, which causes a faster decrease in MR and an acceleration of moisture migration [53,54,137,139,140]. Another conclusion that could be drawn is that the temperature-activated mass transfer diffusion that led to the quick and continuous drop of the *MR* was the cause of the cassava mash weight decrease that was observed during roasting [141].

3.6. Limitations of the study

Despite the remarkable findings, this study has a number of drawbacks. The regulated conditions in the lab-scale setups may not have fully reproduced the unpredictability, non-linear and operational difficulties of real-world systems, such as varying constituent characteristics, changing environmental conditions, human errors and solar irradiance. Scaling up the findings to bigger systems may result in inconsistencies in heat distribution, energy dynamics, and equipment efficiency. These aspects should be taken into account when extrapolating the findings to other industrial or real-life scenarios. Future studies should focus on integrating all probable effects of the roasting processes such as solar energy intermediacy, roasting under different food systems and human to equipment interactions in the machine learning models.

3.7. Conclusion

This research demonstrates a creative and practical approach to improving energy efficiency and energy source diversification and transition from woodfuel based roasting to solar PV. By successfully optimizing the specific energy consumption, temperature and its *RoR*, stirring speed, and duration for roasting cassava mash into gari while maintaining standard quality requirements, this study further highlights the possibilities of promoting sustainable food roasting techniques. The developed processing and quality prediction models fitted very well with the experimental data highlighting their accuracy and application.

Utilizing a random forest regressor model, it has been shown that lab-scale research findings may be effectively used to forecast important design parameters for practical use, including temperature, agitation speed, product quality metrics, and roasting pan geometry. The data showed that enhancing roasting pan geometry specifically increase surface area, improves heat distribution but demands careful balancing to avoid increased energy consumption caused by increased thermal mass. Furthermore, the impacts of initial (ambient) temperatures on the final energy consumption have been highlighted.

The python based machine learning scripts developed in this work offer an invaluable tool for optimizing roasting systems. The random forest scripts can be integrated into design platforms such as solidworks, enabling predictive modeling during the design process and decreasing the need for actual prototypes. Such integration enables the rapid construction of energy-efficient roasting systems adapted to individual, regional and site specific operational requirements.

For the food industry, particularly for the cassava processing into gari, this research has significant implications and impacts such as;

- **Process Optimization:** The findings regarding the optimal roasting duration, stirring speed and temperatures could help processors optimize their operations for efficiency and consistency, reducing waste and increasing quality output. Considering the RoR in roasting processes design could improve the efficiency of both the process and the quality of the products.
- **Product Quality:** The research provides insights into how temperature, RoR, and stirring speed affect the quality parameters of the final product. This could help processors improve the quality of their products, potentially leading to higher customer satisfaction and increased market share.
- **Energy Efficiency:** This research could help food processing companies reduce their energy costs by optimizing the energy consumption during the roasting process, which could lead to increased profitability.
- **Process and Quality Parameters Prediction and Modeling**: The research's ability to develop well-fitting prediction models for the process factors and responses and the use of the Midilli-Kucuk drying kinetic to fit MR data, could provide a valuable tool for predicting the drying behavior of cassava during roasting. This could aid in process, design, control and optimization with the possibility of using Artificial Intelligence (AI) for smart roasting system development. These models could be used for roasting equipment and process designing.
- **Sustainability:** Reducing energy consumption in food processing contributes to industry's sustainability goals. By optimizing energy and resource use, processors and companies can reduce their carbon footprint, contributing to global efforts to combat climate change.
- **Energy transition:** This study focuses on energy transition using creative modeling, practical design solutions, and sustainability principles. It encourages efficient designing of solar energy based roasting systems and serves as part of the templates for incorporating machine learning and energy efficient techniques in the quality food processing industry harmonizing with global initiatives to combat the climate change.

This research could contribute to best practices in the roasting processing industry, leading to improvements in efficiency, product quality, postharvest loss reduction and sustainability. It is a great example of how theoretical scientific research can be transformed into real-life scenarios and dynamic innovation in food industry.

CRediT authorship contribution statement

Mwewa Chikonkolo Mwape: Writing – review & editing, Writing – original draft, Visualization, Validation, Software, Methodology,

Investigation, Formal analysis, Data curation, Conceptualization. **Boris Kulig:** Software, Data curation. **Tina Nurkhoeriyati:** Writing – review & editing, Visualization, Validation, Data curation. **Franz Roman:** Writing – review & editing, Visualization, Validation, Software, Data curation. **Aditya Parmar:** Writing – review & editing, Resources. **Naushad M. Emmambux:** Writing – review & editing, Visualization, Data curation. **Oliver Hensel:** Writing – review & editing, Validation, Supervision, Resources, Project administration, Methodology, Funding acquisition.

Data availability

The authors affirm that the data supporting the study's conclusions are available within the article [and/or] in supplementary materials.

Declaration of competing interest

The authors declare that they have no known competing financial interests or personal relationships that could have appeared to influence the work reported in this paper.

Acknowledgements

The authors gratefully acknowledge financial support for the SUN-GARI project from the German Federal Ministry of Education and Research (Grant code: FKZ 03F0683A) and the European Union's Long-Term Joint European Union-African Union Research and Innovation Partnership on Renewable Energy (LEAP-RE) under grant agreement 963530.

Appendix A. Supplementary data

Supplementary data to this article can be found online at https://doi.org/10.1016/j.tsep.2025.103258.

References

[1] (Food and Agriculture Organization of the United) FAO, 5 facts about food waste and hunger, (2020). https://www.wfp.org/stories/5-facts-about-food-waste-and-hunger (accessed April 9, 2024).
[2] F. Al-juhaimi, K. Ghafoor, M.M. Özcan, M.H.A. Jahurul, E.E. Babiker, S. Jinap, F. Sahena, M.S. Sharifudin, I.S.M. Zaidul, Effect of various food processing and handling methods on preservation of natural antioxidants in fruits and vegetables, J. Food Sci. Technol. 55 (2018) 3872, https://doi.org/10.1007/S13197-018-3370-0.
[3] R.M. Aadil, U. Roobab, A.A. Maan, G.M. Madni, Effect of heat on food properties, Encycl. Food Chem. (2018) 70–75, https://doi.org/10.1016/B978-0-08-100596-5.21660-0.
[4] H. Bin Lim, D.H. Kim, Effects of roasting conditions on physicochemical properties and antioxidant activities in Ginkgo biloba seeds, 1057, Food Sci. Biotechnol. 27 (2018), https://doi.org/10.1007/S10068-018-0348-7.
[5] N.U. Sruthi, Y. Premjit, R. Pandiselvam, A. Kothakota, S.V. Ramesh, An overview of conventional and emerging techniques of roasting: Effect on food bioactive signatures, Food Chem. 348 (2021) 129088, https://doi.org/10.1016/J.FOODCHEM.2021.129088.
[6] T. Nurkhoeriyati, B. Kulig, B. Sturm, O. Hensel, The effect of pre-drying treatment and drying conditions on quality and energy consumption of hot air-dried celeriac slices: optimisation, Foods 10 (2021) 1758, https://doi.org/10.3390/FOODS10081758.
[7] K.S. Youn, H.S. Chung, Optimization of the roasting temperature and time for preparation of coffee-like maize beverage using the response surface methodology, LWT - Food Sci. Technol. 46 (2012) 305–310, https://doi.org/10.1016/J.LWT.2011.09.014.
[8] A. Musa, O.A. Adetola, O.J. Olukunle, A.M. Akintade, Modification and optimization of groundnut (Arachis hypogaea) roasting machine, J. Sci. Res. Reports (2020) 71–83, https://doi.org/10.9734/JSRR/2020/V26I530260.
[9] S.J. Aliyu, J.O. Ojediran, O.D. Oguntoye, G.N. Okon, I. Akinsanya, M.J. Otegbayo, A.A. Banji, Design and fabrication of a peanut roasting machine for commercial use, Int. J. Eng. Trends Technol. 71 (2023) 267–274, https://doi.org/10.14445/22315381/IJETT-V71I9P232.
[10] (Almond Board of California) ABC, Hot Air Roasting of Almonds, (2014). www.almonds.com 〉 2014aq0008_hot_air_roasting_of_almond (accessed November 13, 2024).
[11] C. Chen, R. Khir, Y. Shen, X. Wu, R. Zhang, X. Cao, F. Niederholzer, Z. Pan, Energy consumption and product quality of off-ground harvested almonds under hot air column drying, LWT 138 (2021) 110768, https://doi.org/10.1016/J.LWT.2020.110768.
[12] W. Burton Navicha, Y. Hua, K. Masamba, C. Zhang, Effect of roasting temperatures and times on test parameters used in determination of adequacy of soybean processing, Adv. J. Food Sci. Technol. 13 (2017) 22–28, https://doi.org/10.19026/AJFST.13.3413.
[13] W.B. Navicha, Y. Hua, K. Masamba, X. Kong, C. Zhang, Optimization of soybean roasting parameters in developing nutritious and lipoxygenase free soymilk, J. Food Meas. Charact. 11 (2017) 1899–1908, https://doi.org/10.1007/S11694-017-9572-8.
[14] E. Gibbs, Understanding drum RPM: A roaster's pocket guide, (2022). https://mtpak.coffee/2022/09/understanding-drum-rpm-a-roasters-guide/ (accessed November 14, 2024).
[15] L. Dahdouh, A. Escobar, E. Rondet, J. Ricci, G. Fliedel, L. Adinsi, D. Dufour, B. Cuq, M. Delalonde, Role of dewatering and roasting parameters in the quality of handmade gari, Int. J. Food Sci. Technol. 56 (2021) 1298–1310, https://doi.org/10.1111/ijfs.14745.
[16] M.C. Mwape, A. Parmar, Y. Ouézou Azouma, K. Agboka, H. Hoedt, W. Scheffler, M. Precoppe, N. Mehlomakulu, S. Nkosi, N.M. Emmambux, M. Diale, O. Hensel, Evaluation of Temperature and Energy Requirements for Gari Processing at standard quality parameters in Togo, Tropentag (2023). https://www.tropentag.de/2023/abstracts/posters/420.pdf (accessed February 12, 2024).
[17] W. Quaye, J. Gayin, W.A. Plahar, J. Gayin, I. Yawson, W.A. Plahar, Characteristics of various cassava processing methods and the adoption requirements in Ghana, accessed September 7, 2023, J. Root Crop. 35 (2009) 59–68, https://www.researchgate.net/publication/228308346.
[18] A. Rahayuningtyas, D. Sagita, M.A. Karim, L.E. Yulianti, D.P. Putri, I.F. Azizah, Y. H. Siregar, S.I. Kuala, D.D. Hidayat, A. Darmawan, H. Hariadi, Unraveling the performance of fluidized coffee roasters under slow and fast roasting processes: energy, quality, and economic analysis, J. Biosyst. Eng. 493 (49) (2024) 240–251, https://doi.org/10.1007/S42853-024-00230-3.
[19] D. Lund, Influence of time, temperature, moisture, ingredients, and processing conditions on starch gelatinization, C R C Crit, Rev. Food Sci. Nutr. 20 (1984) 249–273, https://doi.org/10.1080/10408398409527391.
[20] I. Higueras, T. Roldán, J.J. Torrens, eds., Numerical Simulation in Physics and Engineering, 9 (2016). doi: 10.1007/978-3-319-32146-2.
[21] J.-P. Iwuoha, Gari and Cassava production – A small business that can change your life! - Smallstarter Africa, Smallstarter (2013). https://www.smallstarter.com/browse-ideas/gari-and-cassava-production/ (accessed October 6, 2023).
[22] A. Burns, R. Gleadow, J. Cliff, A. Zacarias, T. Cavagnaro, Cassava: the drought, war and famine crop in a changing world, Sustainability 2 (2010) 3572–3607, https://doi.org/10.3390/su2113572.
[23] G.E. Shackelford, N.R. Haddaway, H.O. Usieta, P. Pypers, S.O. Petrovan, W. J. Sutherland, Cassava farming practices and their agricultural and environmental impacts: A systematic map protocol, Environ. Evid. 7 (2018) 1–7, https://doi.org/10.1186/S13750-018-0142-2/TABLES/1.
[24] P.P. Das, P. Duarah, M.K. Purkait, Fundamentals of food roasting process, High-Temperature Process, Food Prod. Unit Oper Process. Equip. Food Ind. (2023) 103–130, https://doi.org/10.1016/B978-0-12-818618-3.00005-7.
[25] L. Rani, M. Kumar, D. Kaushik, J. Kaur, A. Kumar, F. Oz, C. Proestos, E. Oz, A review on the frying process: Methods, models and their mechanism and application in the food industry, Food Res. Int. 172 (2023) 113176, https://doi.org/10.1016/J.FOODRES.2023.113176.
[26] J.H. Bradbury, A.P. Cardoso, E. Mirione, M. Ernesto, F. Massaza, J. Cliff, M. R. Haque, Processing of cassava roots to remove cyanogens, J. Food Compos. Anal. 18 (2005) 451–460, https://doi.org/10.1016/j.jfca.2004.04.002.
[27] E.A. Nainggolan, J. Banout, K. Urbanova, Recent trends in the pre-drying, drying, and post-drying processes for cassava tuber: a review, Foods 13 (2024) 1778, https://doi.org/10.3390/FOODS13111778.
[28] S. Ambawat, A. Sharma, R.K. Saini, Mathematical modeling of thin layer drying kinetics and moisture diffusivity study of pretreated moringa oleifera leaves using fluidized bed dryer, Process. 2022, Vol. 10, Page 2464 10 (2022) 2464. doi: 10.3390/PR10112464.
[29] A. Ahmad, O. Prakash, A. Kumar, Drying kinetics and economic analysis of bitter gourd flakes drying inside hybrid greenhouse dryer, Environ. Sci. Pollut. Res. 30 (2023) 72026–72040, https://doi.org/10.1007/S11356-021-17044-X/TABLES/11.
[30] R. Fadhil, S. Safrizal, K. Rizal, B.S. Putra, J. Firmansyah, Study of variations in the roasting time of gayo arabica coffee in the drying phase, Coffee Sci. 18 (2023), https://doi.org/10.25186/.V18I.2085.
[31] Nucleus, Rate Of Rise (RoR) : When It's Useful For Coffee Roasting, (2024). https://nucleuscoffee.com/en/blogs/cafe/rate-of-rise (accessed July 9, 2024).
[32] O. Bongomin, A. Yemane, B. Kembabazi, C. Malanda, M. Chikonkolo Mwape, N. Sheron Mpofu, D. Tigalana, Industry 4.0 disruption and its neologisms in major industrial sectors: A state of the art, J. Eng. 2020 (2020) 1–45, https://doi.org/10.1155/2020/8090521.
[33] S. Raut, G. von Gersdorff, J. Schemminger, J. Adolphs, B. Sturm, Improving food processing through integration of artificial intelligence in the drying process: a perspective, in: 42. GIL-Jahrestagung, Künstliche Intelligenz Der Agrar. Und Ernährungswirtschaft, 2022, pp. 231–236, https://dl.gi.de/handle/20.500.12116/38402 (accessed August 9, 2024).
[34] M.C. Mwape, N.S. Mpofu, C.H. Malanda, I.K. Kimutai, Early impacts of COVID-19 pandemic on the crude oil prices and demand in sub-Saharan Africa: A review, Int. J. Energy Res. 2024 (2024) 5548311, https://doi.org/10.1155/2024/5548311.

[35] Y. Lv, Transitioning to sustainable energy: opportunities, challenges, and the potential of blockchain technology, Front. Energy Res. 11 (2023) 1258044, https://doi.org/10.3389/FENRG.2023.1258044/BIBTEX.

[36] T. Kondakci, W. Zhou, Recent applications of advanced control techniques in food industry, Food Bioprocess Technol. 103 (10) (2016) 522–542, https://doi.org/10.1007/S11947-016-1831-X.

[37] M.I.H. Khan, S.S. Sablani, R. Nayak, Y. Gu, Machine learning-based modeling in food processing applications: State of the art, Compr. Rev. Food Sci. Food Saf. 21 (2022) 1409–1438, https://doi.org/10.1111/1541-4337.12912.

[38] M.C. Mwape, A. Parmar, F. Roman, Y.O. Azouma, N.M. Emmambux, O. Hensel, Determination and Modeling of Proximate and Thermal Properties of De-Watered Cassava Mash (Manihot esculenta Crantz) and Gari (Gelatinized cassava mash) Traditionally Processed (In Situ) in Togo, Energies 16 (2023) 6836, https://doi.org/10.3390/EN16196836.

[39] C. Felber, Y.O. Azouma, M. Reppich, Evaluation of analytical methods for the determination of the physicochemical properties of fermented, granulated, and roasted cassava pulp - gari, Food Sci. Nutr. 5 (2017) 46–53, https://doi.org/10.1002/fsn3.363.

[40] S.S. Sobowale, J.A. Adebiyi, O.A. Adebo, Design, construction, and performance evaluation of a gari roaster, J. Food Process Eng. 40 (2017), https://doi.org/10.1111/jfpe.12493.

[41] F. Mansouri, A. Allay, A. Ben Moumen, C. Benkirane, Y. Taaifi, K. Belhaj, M. Addi, C. Hano, M.L. Fauconnier, H.S. Caid, A. Elamrani, Laboratory-scale optimization of hemp seed roasting temperature and time for producing a high-quality pressed oil, J. Food Process. Preserv. 2023 (2023), https://doi.org/10.1155/2023/8261279.

[42] S. Reyniers, N. De Brier, K. Brijs, B. De Ketelaere, W. Akkermans, S. Matthijs, J. A. Delcour, P. Goos, I-optimal design of split-plot mixture-process variable experiments: A case study on potato crisps, Food Qual. Prefer. 101 (2022) 104620, https://doi.org/10.1016/J.FOODQUAL.2022.104620.

[43] (Cereals & Grains Association) CGA, Approved Methods of Analysis, (2023). https://www.cerealsgrains.org/resources/methods/Pages/default.aspx (accessed February 7, 2023).

[44] M. Özdemir, O. Devres, Analysis of color development during roasting of hazelnuts using response surface methodology, J. Food Eng. 45 (2000) 17–24, https://doi.org/10.1016/S0260-8774(00)00036-4.

[45] S. Sun, G. Li, H. Chen, Y. Guo, J. Wang, Q. Huang, W. Hu, Optimization of support vector regression model based on outlier detection methods for predicting electricity consumption of a public building WSHP system, Energy Build. 151 (2017) 35–44, https://doi.org/10.1016/J.ENBUILD.2017.06.056.

[46] Y. Wang, Y. Zhang, F. Zhang, J. Yi, Robust quadratic regression and its application to energy-growth consumption problem, Math. Probl. Eng. 2013 (2013), https://doi.org/10.1155/2013/210510.

[47] J. Luo, T. Hong, S.C. Fang, Robust regression models for load forecasting, IEEE Trans. Smart Grid 10 (2018) 5397–5404, https://doi.org/10.1109/TSG.2018.2881562.

[48] R.K. Raigar, R. Upadhyay, H.N. Mishra, Optimization of microwave roasting of peanuts and evaluation of its physicochemical and sensory attributes, J. Food Sci. Technol. 54 (2017) 2145–2155, https://doi.org/10.1007/S13197-017-2654-0/FIGURES/3.

[49] J. Gutiérrez, E.L. Chica, J.F. Pérez, Parametric analysis of a gasification-based cookstove as a function of biomass density, gasification behavior, airflow ratio, and design, ACS Omega 7 (2022) 7481–7498, https://doi.org/10.1021/ACSOMEGA.1C05137/ASSET/IMAGES/MEDIUM/AO1C05137_M006.GIF.

[50] S. Suherman, E.E. Susanto, A.W. Zardani, N.H.R. Dewi, H. Hadiyanto, Energy–exergy analysis and mathematical modeling of cassava starch drying using a hybrid solar dryer, Cogent Eng. 7 (2020), https://doi.org/10.1080/23311916.2020.1771819.

[51] S. Zhao, Z. Yao, B. Ma, X. Li, C. Wang, Phase transformation and roasting kinetics of vanadium slag in air atmosphere, J. Ind. Eng. Chem. 133 (2024) 195–206, https://doi.org/10.1016/j.jiec.2023.11.058.

[52] K.R. Uren, J. Vosloo, A.F. van der Merwe, G. van Schoor, Heat and mass transfer modeling of an artisan coffee roasting process: A comparative study, Dry. Technol. 41 (2023) 1697–1713, https://doi.org/10.1080/07373937.2023.2175851.

[53] L. Bennamoun, M.C. Ndukwu, Modeling and simulation of drying kinetics/curves: application to building materials, J. Build. Pathol. Rehabil. 7 (2022) 1–15, https://doi.org/10.1007/S41024-021-00143-0/FIGURES/14.

[54] M. Reppich, Z. Jegla, J. Grondinger, Y.O. Azouma, V. Turek, Mathematical Modeling of drying processes of selected fruits and vegetables, Chem.-Ing.-Tech. 93 (2021) 1581–1589, https://doi.org/10.1002/CITE.202100029.

[55] F. Román, O. Hensel, Effect of air temperature and relative humidity on the thin-layer drying of celery leaves (Apium graveolens var. secalinum), Agric. Eng. Int. CIGR J. 13 (2011) https://cigrjournal.org/index.php/Ejounral/article/view/1876 (accessed April 25, 2024).

[56] A. Midilli, H. Kucuk, Z. Yapar, A new model for single-layer drying, Dry. Technol. 20 (2002) 1503–1513, https://doi.org/10.1081/DRT-120005864.

[57] Y.C. Agrawal, R.P. Singh, Thin-layer drying studies on short-grain rice, ASAE Pap. (1978) 77–3531.

[58] W.K. Lewis, The rate of drying of solid materials, Ind. Eng. Chem. 13 (1921) 427–432, https://doi.org/10.1021/IE50137A021.

[59] G.Y. Wang, R. Singh, A single layer drying equation for rough rice, ASAE Pap. (1978) 78–3001.

[60] A. Fabbri, C. Cevoli, L. Alessandrini, S. Romani, Numerical modeling of heat and mass transfer during coffee roasting process, J. Food Eng. 105 (2011) 264–269, https://doi.org/10.1016/J.JFOODENG.2011.02.030.

[61] J.B. Hutchings, Food Colour and Appearance, Food Colour Appear. (1994), https://doi.org/10.1007/978-1-4615-2123-5.

[62] N. Li, B. Zhang, S. Zhao, M. Niu, C. Jia, Q. Huang, Y. Liu, Q. Lin, Influence of Lactobacillus/Candida fermentation on the starch structure of rice and the related noodle features, Int. J. Biol. Macromol. 121 (2019) 882–888, https://doi.org/10.1016/J.IJBIOMAC.2018.10.097.

[63] L. Day, M. Golding, Food structure, rheology, and texture, Encycl. Food Chem. (2016) 125–129, https://doi.org/10.1016/B978-0-08-100596-5.03412-0.

[64] A. Andrés-Bello, V. Barreto-Palacios, P. García-Segovia, J. Mir-Bel, J. Martínez-Monzó, Effect of pH on color and texture of food products, Food Eng. Rev. 5 (2013) 158–170, https://doi.org/10.1007/S12393-013-9067-2/METRICS.

[65] O. Olaosebikan, A. Bello, K. de Sousa, R. Ndjouenkeu, M. Adesokan, E. Alamu, A. Agbona, J. Van Etten, F.N. Kégah, D. Dufour, A. Bouniol, B. Teeken, Drivers of consumer acceptability of cassava gari-eba food products across cultural and environmental settings using the triadic comparison of technologies approach (tricot), J. Sci. Food Agric. 104 (2024) 4770–4781, https://doi.org/10.1002/JSFA.12867.

[66] (Commission Internationale de ÍEclairage) CIE, International Standards | CIE, (2024). https://cie.co.at/publications/international-standards (accessed May 13, 2024).

[67] T. Kahyaoglu, Optimization of the pistachio nut roasting process using response surface methodology and gene expression programming, LWT 41 (2008) 26–33, https://doi.org/10.1016/J.LWT.2007.03.026.

[68] (Food and Agriculture Organization of the United) FAO, FAO publications catalogue 2023, FAO Publ. Cat. 2023 (2023). doi: 10.4060/CC7285EN.

[69] I. Oduro, W.O. Ellis, N.T. Dziedzoave, K. Nimako-Yeboah, Quality of gari from selected processing zones in Ghana, Food Control 11 (2000) 297–303, https://doi.org/10.1016/S0956-7135(99)00106-1.

[70] J.A. Montagnac, C.R. Davis, S.A. Tanumihardjo, Nutritional value of cassava for use as a staple food and recent advances for improvement, Compr. Rev. Food Sci. Food Saf. 8 (2009) 181–194, https://doi.org/10.1111/j.1541-4337.2009.00077.x.

[71] G.A. Adeyemi, D. Muhammed, R.A. Adenike, B.O. Ogbori, Yield, suitability and sensory evaluation of gari produced from two cassava varieties at different age | international journal of natural sciences: current and future research trends, Int. J. Nat. Sci. Curr. Futur. Res Trends (2020) https://ijnscfrtjournal.isrra.org/index.php/Natural_Sciences_Journal/article/view/1029 (accessed March 4, 2022.

[72] R.S. Amoah, L.K. Sam-Amoah, C.A. Boahen, F. Duah, Estimation of the material losses and gari recovery rate during the processing of varieties and ages of cassava into gari, Asian, J. Agric. Res. 4 (2010) 71–79, https://doi.org/10.3923/ajar.2010.71.79.

[73] S. Henderson, R. Perry, Agricultural process engineering., 1976. https://www.cabidigitallibrary.org/doi/full/10.5555/19771460529 (accessed May 13, 2024).

[74] JMP, How to Use the Desirability Function, Support/Help (2024). https://www.jmp.com/support/help/en/18.0/index.shtml#page/jmp/how-to-use-the-desirability-function.shtml (accessed June 5, 2024).

[75] R.D. Riley, L. Archer, K.I.E. Snell, J. Ensor, P. Dhiman, G.P. Martin, L.J. Bonnett, G.S. Collins, Evaluation of clinical prediction models (part 2): how to undertake an external validation study, BMJ 384 (2024), https://doi.org/10.1136/BMJ-2023-074820.

[76] S.F. Zandrazavi, M. Shafie-khah, M. Pashaei, Data-driven optimal scheduling of isolated microgrid using random forest regressor, in: 2024 IEEE Int. Conf. Environ. Electr. Eng. 2024 IEEE Ind. Commer. Power Syst. Eur. (EEEIC / I&CPS Eur., 2024, pp. 1–6, 10.1109/EEEIC/ICPSEUROPE61470.2024.10751201.

[77] T. Fujii, M. Sako, K. Ishihama, Y. Kohno, T. Makino, N. Yasuo, S. Kawauchi, Prediction of CO2 absorbing performance of amine aqueous solution using random forest models, Gas Sci. Eng. 129 (2024) 205417, https://doi.org/10.1016/J.JGSCE.2024.205417.

[78] A.P. Brincoveanu, E. Fiorentis, R. Plamanescu, A.M. Dumitrescu, M. Albu, Estimation of the LV power profiles variability using the Goodness of Fit approach. 2024 14th IEEE Int. Work. Appl. Meas. Power Syst. AMPS 2024 - Proc., 2024 doi: 10.1109/AMPS62611.2024.10706674.

[79] K.R. Mehta, K. Jayant Naidu, M. Baheti, D. Parmar, A. Sharmila, Internet of things based smart irrigation system using ESP WROOM 32, J. Internet Things 5 (2023) 45–55, https://doi.org/10.32604/JIOT.2023.043102.

[80] L.H.B. Santos, E.J.M. da Silva, A.A. de Oliveira Farias, J.F. dos Santos, I.R.M. R. Morais, W. da Silva Fonseca, M. de Oliveira e Silva, Monitoring industrial systems using ESP-NOW protocol with Mesh and Ad Hoc network, in: 2023 15th IEEE Int. Conf. Ind. Appl. INDUSCON 2023 - Proc., 2023, pp. 559–566, 10.1109/INDUSCON58041.2023.10374804.

[81] S.O. Jekayinfa, J.O. Olajide, Analysis of energy usage in the production of three selected cassava-based foods in Nigeria, J. Food Eng. 82 (2007) 217–226, https://doi.org/10.1016/J.JFOODENG.2007.02.003.

[82] M.A. Mansournia, R. Waters, M. Nazemipour, M. Bland, D.G. Altman, Bland-Altman methods for comparing methods of measurement and response to criticisms, Glob. Epidemiol. 3 (2021) 100045, https://doi.org/10.1016/J.GLOEPI.2020.100045.

[83] Y. Zhou, Y. Zhu, W.K. Wong, Statistical tests for homogeneity of variance for clinical trials and recommendations, Contemp. Clin. Trials Commun. 33 (2023) 101119, https://doi.org/10.1016/J.CONCTC.2023.101119.

[84] H. An, E.E. Langas, A.S. Gill, Effect of scanning speed, scanning pattern, and tip size on the accuracy of intraoral digital scans, J. Prosthet. Dent. 131 (2024) 1160–1167, https://doi.org/10.1016/J.PROSDENT.2022.05.005.

[85] P.P. Das, P. Duarah, M.K. Purkait, Fundamentals of food roasting process, High-Temperature Process. Food, Prod. (2023) 103–130, https://doi.org/10.1016/B978-0-12-818618-3.00005-7.

[86] L.L. Pereira, D.G. Debona, P.F. Pinheiro, G.F. de Oliveira, C.S. ten Caten, V. Moksunova, A.V. Kopanina, I.I. Vlasova, A.I. Talskikh, H. Yamamoto, Roasting process, Food Eng. Ser. (2021) 303–372, https://doi.org/10.1007/978-3-030-54437-9_7/FIGURES/59.
[87] P. Goos, M. David, Statistics with JMP: Hypothesis Tests, ANOVA and Regression - Peter Goos, David Meintrup - Google Books, (2016). https://books.google.de/books?hl=en&lr=&id=hYuXCwAAQBAJ&oi=fnd&pg=PP1&dq=limited+variability+in+data+analysis+statistics+JMP&ots=Gab8Pt5vf0&sig=IuHngNWz_jjDr1SbP75rs1Y58Mg&redir_esc=y#v=onepage&q&f=false (accessed August 8, 2024).
[88] M. Rojas, A. Hommes, H.J. Heeres, F. Chejne, Physicochemical phenomena in the roasting of cocoa (Theobroma cacao L.), Food Eng. Rev. 143 (14) (2021) 509–533, https://doi.org/10.1007/S12393-021-09301-Z.
[89] M. Fikry, Y.A. Yusof, A.M. Al-Awaadh, R.A. Rahman, N.L. Chin, E. Mousa, L. S. Chang, Effect of the roasting conditions on the physicochemical, quality and sensory attributes of coffee-like powder and brew from defatted palm date seeds, Foods 8 (2019) 61, https://doi.org/10.3390/FOODS8020061.
[90] P.B. Pathare, A.P. Roskilly, Quality and energy evaluation in meat cooking, Food Eng. Rev. 84 (8) (2016) 435–447, https://doi.org/10.1007/S12393-016-9143-5.
[91] L. Lu, C.M. Anderson-Cook, T.J. Robinson, Optimization of designed experiments based on multiple criteria utilizing a pareto frontier, Technometrics 53 (2011) 353–365, https://doi.org/10.1198/TECH.2011.10087.
[92] D.A. Iancu, N. Trichakis, Pareto Efficiency in Robust Optimization, doi: 10.1287/Mnsc.2013.1753 60 (2013) 130–147. doi: 10.1287/MNSC.2013.1753.
[93] L. Wang, Energy efficiency technologies for sustainable food processing, Energy Effic. 7 (2014) 791–810, https://doi.org/10.1007/S12053-014-9256-8/TABLES/4.
[94] (Food and Agriculture Organization of the United) FAO, Global Food Losses and Food Waste – Extent, Causes and Prevention, Sustain. Food Value Chain. Knowl. Platf. (2024). https://www.fao.org/sustainable-food-value-chains/library/details/en/c/266053/ (accessed August 9, 2024).
[95] H. Feng, Y. Yin, J. Tang, Microwave drying of food and agricultural materials: basics and heat and mass transfer modeling, Food Eng. Rev. 4 (2012) 89–106, https://doi.org/10.1007/S12393-012-9048-X/TABLES/3.
[96] S. Agrawal, T. Simon, M. North, T. Cui, An experimental study on the effects of agitation on convective heat transfer, Int. J. Heat Mass Transf. 90 (2015) 302–313, https://doi.org/10.1016/J.IJHEATMASSTRANSFER.2015.05.105.
[97] A. Ma, T. Xie, G. Li, X. Zheng, L. Zhang, J. Peng, Dechlorination of zinc oxide dust by microwave roasting with RSM optimization, Miner. Met. Mater. Ser. Part F 10 (2018) 715–723, https://doi.org/10.1007/978-3-319-72138-5_68/FIGURES/4.
[98] R. Jeantet, P. Schuck, T. Six, C. Andre, G. Delaplace, The influence of stirring speed, temperature and solid concentration on the rehydration time of micellar casein powder, Dairy, Sci. Technol. 902 (90) (2009) 225–236, https://doi.org/10.1051/DST/2009043.
[99] V.R. Mehta, · Mayur, P. Sutaria, investigation on the effect of stirring process parameters on the dispersion of SiC particles inside melting crucible, 27 (2021) 2989–3002. doi: 10.1007/s12540-020-00612-0.
[100] L.L. Pereira, T.R. Moreira, Quality determinants in coffee production, (2021). doi: 10.1007/978-3-030-54437-9.
[101] P. Goos, M. David, Effect heredity, (2016). https://www.jmp.com/support/help/en/18.0/index.shtml#page/jmp/effect-heredity.shtml (accessed August 2, 2024).
[102] H. Xu, H. Hu, C. Zhang, W. Xue, T. Li, X. Zhang, L. Wang, Properties of pyrodextrinization corn starch and their inhibitory effect on the retrogradation of fresh rice noodles, Int. J. Biol. Macromol. 257 (2024) 128555, https://doi.org/10.1016/J.IJBIOMAC.2023.128555.
[103] K.V. Murthy, R. Ravi, K.K. Bhat, K.S.M.S. Raghavarao, Studies on roasting of wheat using fluidized bed roaster, J. Food Eng. 89 (2008) 336–342, https://doi.org/10.1016/J.JFOODENG.2008.05.014.
[104] M. Li, V.D. Daygon, V. Solah, S. Dhital, Starch granule size: Does it matter? Crit. Rev. Food Sci. Nutr. 63 (2023) 3683–3703, https://doi.org/10.1080/10408398.2021.1992607.
[105] Y. Ai, J. Lin Jane, Understanding starch structure and functionality, Starch Food Struct. Funct. Appl. (2018) 151–178, https://doi.org/10.1016/B978-0-08-100868-3.00003-2.
[106] A. Escobar, L. Dahdouh, E. Rondet, J. Ricci, D. Dufour, T. Tran, B. Cuq, M. Delalonde, Development of a novel integrated approach to monitor processing of cassava roots into gari: macroscopic and microscopic scales, Food Bioprocess Technol. 11 (2018) 1370–1380, https://doi.org/10.1007/S11947-018-2106-5/TABLES/5.
[107] J. Ndisya, D. Mbuge, B. Kulig, A. Gitau, O. Hensel, B. Sturm, Hot air drying of purple-speckled Cocoyam (Colocasia esculenta (L.) Schott) slices: Optimisation of drying conditions for improved product quality and energy savings, Therm. Sci. Eng. Prog. 18 (2020) 100557, https://doi.org/10.1016/J.TSEP.2020.100557.
[108] (WorldBank) WB, Scaling-Up Access to Clean Cooking Technologies and Fuels in Sub-Saharan Africa Africa Clean Cooking Energy Solutions Initiative, 2017. https://www.esmap.org/node/71158.
[109] S.H.B. Mundarinti, H.A. Ahad, Impact of Pistacia lentiscus plant gum on particle size and swelling index in central composite designed Amoxycillin Trihydrate mucoadhesive microspheres, Indian J. Pharm Educ. Res. 57 (2023) 763–772, https://doi.org/10.5530/IJPER.57.3.93.
[110] D.M.T.E. Ali, V. Motuzienė, R. Džiugaitė-Tumėnienė, AI-driven innovations in building energy management systems: a review of potential applications and energy savings, Energies (2024) 4277, https://doi.org/10.3390/EN17174277.
[111] I.W. Árpád, J.T. Kiss, D. Kocsis, Role of the volume-specific surface area in heat transfer objects: A critical thinking-based investigation of Newton's law of cooling, Int. J. Heat Mass Transf. 227 (2024) 125535, https://doi.org/10.1016/J.IJHEATMASSTRANSFER.2024.125535.
[112] B. Aksüt, H. Polatcı, M. Taşova, The effect of pre-treatment and drying temperatures on energy consumption and quality characteristics in drying of lemon (Citrus limon L.) slices, J. Therm. Anal. Calorim. 148 (2023) 10415–10427, https://doi.org/10.1007/S10973-023-12362-3/TABLES/6.
[113] A.B. Aurelie Bechoff, K.I.T. Keith, I. Tomlins, U.C. Ugo Chijioke, P.I. Paul Ilona, B. B. Ben Bennett, A.W. Andrew Westby, E.B. Erick Boy, Variability in traditional processing of gari: a major food security product from cassava, Food Chain 8 (2019) 39–57, https://doi.org/10.3362/2046-1887.18-00015.
[114] H. Ecker, N.B. Adams, M. Schmitz, W.A. Wetsch, Feasibility of real-time compression frequency and compression depth assessment in CPR using a "machine-learning" artificial intelligence tool, Resusc. plus 20 (2024) 100825, https://doi.org/10.1016/J.RESPLU.2024.100825.
[115] A. Sabiniewicz, S. Wittig, A. Haehner, C. Müller, C. Galvao, M. Nakanishi, T. Hummel, The digital scent device 20: an automated, self-administered odor identification test, Eur. Arch. Oto-Rhino-Laryngology 281 (2024) 6661–6668, https://doi.org/10.1007/S00405-024-08887-4/FIGURES/5.
[116] V. Illera-Domínguez, X. Font-Aragonés, V. Toro-Román, S. Díaz-Alejandre, C. Pérez-Chirinos, L. Albesa-Albiol, S. González-Millán, B. Fernández-Valdés, Validity of force and power measures from an integrated rotary encoder in a handygym portable flywheel exercise device, Appl. Sci. 14 (2024) 9832, https://doi.org/10.3390/APP14219832/S1.
[117] A.S. Mujumdar, Handbook of Industrial Drying, Fourth, Taylor & Francis Group, London, 2015, 10.1080/07373930701399224.
[118] P. Lehmann, S. Assouline, D. Or, Characteristic lengths affecting evaporative drying of porous media, Phys. Rev. E - Stat. Nonlinear, Soft Matter Phys. 77 (2008) 056309, https://doi.org/10.1103/PHYSREVE.77.056309/FIGURES/13/MEDIUM.
[119] A.S. Mujumdar, A.S. Menon, Drying of solids: principles, classification, and selection of dryers, Handb. Ind. Dry. (2020) 1–39, https://doi.org/10.1201/9780429289774-1.
[120] M. Pateiro, M. Vargas-Ramella, D. Franco, A. Gomes da Cruz, G. Zengin, M. Kumar, K. Dhama, J.M. Lorenzo, The role of emerging technologies in the dehydration of berries: Quality, bioactive compounds, and shelf life, Food Chem. X 16 (2022) 100465, https://doi.org/10.1016/J.FOCHX.2022.100465.
[121] G. Chen, W. Wang, A.S. Mujumdar, Theoretical study of microwave heating patterns on batch fluidized bed drying of porous material, Chem. Eng. Sci. 56 (2001) 6823–6835, https://doi.org/10.1016/S0009-2509(01)00320-7.
[122] F. Fathi, S.N. Ebrahimi, L.C. Matos, M.B.P.P. Oliveira, R.C. Alves, Emerging drying techniques for food safety and quality: A review, Compr. Rev. Food Sci. Food Saf. 21 (2022) 1125–1160, https://doi.org/10.1111/1541-4337.12898.
[123] F. Zhu, Composition, structure, physicochemical properties, and modifications of cassava starch, Carbohydr. Polym. 122 (2015) 456–480, https://doi.org/10.1016/j.carbpol.2014.10.063.
[124] A. Gevaudan, G. Chuzel, S. Didier, J. Andrieu, Physical properties of cassava mash, Int. J. Food Sci. Technol. 24 (1989) 637–645, https://doi.org/10.1111/j.1365-2621.1989.tb00690.x.
[125] U. Ulyarti, L. Lisani, S. Surhaini, P. Lumbanraja, B. Satrio, S. Supriyadi, N. Nazarudin, The application of gelatinisation techniques in modification of cassava and yam starches using precipitation method, J. Food Sci. Technol. 59 (2022) 1230–1238, https://doi.org/10.1007/S13197-021-05134-0/FIGURES/5.
[126] A.S. Olanrewaju, Effects of garification (roasting) duration on the quality characteristics of cassava gari, Ann. Food Sci. Technol. (2016) https://www.researchgate.net/publication/319839906_EFFECT_OF_GARIFICATION_ROASTING_DURATION_ON_THE_QUALITY_CHARACTERISTICS_OF_CASSAVA_GARI (accessed November 11, 2022.
[127] G. Xanthopoulos, N. Oikonomou, G. Lambrinos, Applicability of a single-layer drying model to predict the drying rate of whole figs, J. Food Eng. 81 (2007) 553–559, https://doi.org/10.1016/J.JFOODENG.2006.11.033.
[128] I.T. Toĝrul, D. Pehlivan, Modelling of thin layer drying kinetics of some fruits under open-air sun drying process, J. Food Eng. 65 (2004) 413–425, https://doi.org/10.1016/J.JFOODENG.2004.02.001.
[129] O. Taşkin, G. İzli, N. İzli, Convective drying kinetics and quality parameters of european cranberrybush, Tarım Bilim. Derg. 24 (2018) 349–358, https://doi.org/10.15832/ANKUTBD.456654.
[130] O. Taskin, A. Polat, A.B. Etemoglu, N. Izli, Energy and exergy analysis, drying kinetics, modeling, microstructure and thermal properties of convective-dried banana slices, J. Therm. Anal. Calorim. 147 (2022) 2343–2351, https://doi.org/10.1007/S10973-021-10639-Z/FIGURES/10.
[131] M. Shimpy, A. Kumar, R.K. Kumar, H. Sahdev, Manchanda, Comparison of groundnut drying in simple and modified natural convection greenhouse dryers: Thermal, environmental and kinetic analyses, J. Stored Prod. Res. 98 (2022) 101990, https://doi.org/10.1016/J.JSPR.2022.101990.
[132] T. Gunhan, V. Demir, E. Hancioglu, A. Hepbasli, Mathematical modelling of drying of bay leaves, Energy Convers. Manag. 46 (2005) 1667–1679, https://doi.org/10.1016/J.ENCONMAN.2004.10.001.
[133] Q. Zhang, Y. Song, X. Wang, … W.Z.-C.-J. of, undefined 2016, Mathematical modeling of debittered apricot (Prunus armeniaca L.) kernels during thin-layer drying, Taylor Fr. Zhang, Y Song, X Wang, WQ Zhao, XH FanCyTA-Journal Food, 2016•Taylor Fr. 14 (2016) 509–517. doi: 10.1080/19476337.2015.1136843.
[134] A. Silva, F. Almeida, E. Lima, … F.S.-C.-J. of, undefined 2008, Drying kinetics of coriander (Coriandrum sativum) leaf and stem cinéticas de secado de hoja y tallo de cilantro (Coriandrum sativum), Taylor Fr. Silva, FAC Almeida, EE Lima, FLH Silva, JP GomesCYTA-Journal Food, 2008 Taylor Fr. 6 (2008) 13–19. doi: 10.1080/11358120809487622.

[135] L.A. Mohamed, M. Kouhila, A. Jamali, S. Lahsasni, N. Kechaou, M. Mahrouz, Single layer solar drying behaviour of citrus aurantium leaves under forced convection, Energy Convers. Manag. 46 (2005) 1473–1483, https://doi.org/10.1016/J.ENCONMAN.2004.08.001.
[136] D. Evin, Thin layer drying kinetics of Gundelia tournefortii L, Food Bioprod. Process. 90 (2012) 323–332, https://doi.org/10.1016/J.FBP.2011.07.002.
[137] J. Jiang, L. Dang, H. Tan, B. Pan, H. Wei, Thin layer drying kinetics of pregelatinized starch under microwave, J. Taiwan Inst. Chem. Eng. 72 (2017) 10–18, https://doi.org/10.1016/j.jtice.2017.01.005.
[138] W.A.M. McMinn, Thin-layer modelling of the convective, microwave, microwave-convective and microwave-vacuum drying of lactose powder, J. Food Eng. 72 (2006) 113–123, https://doi.org/10.1016/J.JFOODENG.2004.11.025.
[139] M. Zielinska, M. Markowski, Air drying characteristics and moisture diffusivity of carrots, Chem. Eng. Process. Process Intensif. 49 (2010) 212–218, https://doi.org/10.1016/J.CEP.2009.12.005.
[140] T.D. Karapantsios, Conductive drying kinetics of pregelatinized starch thin films, (2005). doi: 10.1016/j.jfoodeng.2005.05.047.
[141] K. Abbas, A. Saleh, O. Lasekan, S.K. Khalil, A review on factors affecting drying process of pistachio and their impact on product's quality., (2010).